Frequency analysis of non-uniform bolted beams

Bimal Purohit

A Thesis Submitted to

Indian Institute of Technology Hyderabad

In Partial Fulfillment of the Requirements for

The Degree of Master of Technology

भारतीय प्रौद्योगिकी संस्थान हैदराबाद
Indian Institute of Technology Hyderabad

Department of Mechanical Engineering

June 2015

Declaration

I declare that this written submission represents my ideas in my own words, and where ideas or words of others have been included, I have adequately cited and referenced the original sources. I also declare that I have adhered to all principles of academic honesty and integrity and have not misrepresented or fabricated or falsified any idea/data/fact/source in my submission. I understand that any violation of the above will be a cause for disciplinary action by the Institute and can also evoke penal action from the sources that have thus not been properly cited, or from whom proper permission has not been taken when needed.
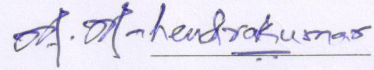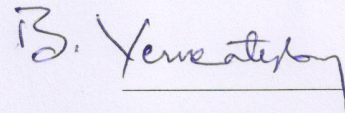
(Signature)

Bimal Purohit

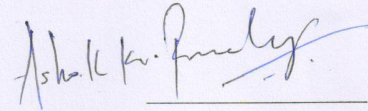(Bimal Purohit)

ME13M1005

(Roll No.)

Approval Sheet

This Thesis entitled "Frequency analysis of non-uniform bolted beams" by Bimal Purohit is approved for the degree of Master of Technology from IIT Hyderabad

(Dr. Mahendra Kumar Madhavan) Examiner
Dept. of Civil Eng
IITH

(Dr. B. Venkatesham) Examiner
Dept. Mech. Eng.
IITH

(Dr. Ashok Kr. Pandey) Adviser
Dept. of Mech. Eng
IITH

Acknowledgements

Dedication

Dedicated To

My beloved parents

(Mr. G.C Purohit and Mrs. Beena Purohit)

Abstract

Modal analysis of non-uniform bolted structures are of critical significance in modeling many complex mechanical structures such as airplanes, missiles, ships, etc. The study of vibration is of foremost importance when it comes to mechanical and aerospace applications. The vibration measurement is a powerful but a sophisticated tool for designing mechanical structures. It helps to unravel critical system dynamics and hence designing the model in a better way. The use of joints is important for a mechanical structure as due to its compatibility and access. A seamless mechanical structure of large dimensions is difficult to be made hence the use of joints is required. There are vast literatures available related with the analytical as well as numerical modeling of bolted joint. The bolted joints are classified on the basis of frictional force, extension of joint, loading, etc. There exist different models like Iwan model, Bou-Wen model, etc for modeling of bolted joint. For our case we take the bolted joint as a torsional spring with no damping effect. The use of torsional spring is inspired by the mechanics of the studied structure. The torsional spring takes care of the moment that is transferred at the joint and as there is no axial force acting at the joint the need of linear spring is not required. However, most of the analytical model discuss about the modeling of first mode of uniform structures with bolted joint. In this thesis, we present the modeling of single as well as bolted non-uniform beams using approximate mode shapes for higher modes. To develop the model, we first studied a simply supported beam using approximate mode shape method. The study is done for obtaining higher modes of single non-uniform beams and then the work is extended for bolted beams with three sections. The results are verified using numerical study. We present the study for second and third vibrational modes as compared to previous works for first mode.

Then we extended our study to beams with cantilever configuration which is important to structure with fixed free boundary conditions. The modal analysis is done for the first three fundamental modes. We carried out experiments to measure the modal frequencies and shapes of the test structures. Polytec. Vibrometer is used for the experimental study and capturing first three modes. It uses the doppler effect principle to capture the vibrational modes. The beams are made of Aluminum material and have same dimensions. Subsequently, we also did numerical modeling of non-uniform beams in ANSYS to verify the validity of the Euler-Bernoulli beam theory in developing the analytical models. Finally, using the Euler-Bernoulli beam theory, we obtain the analytical mode shapes using the approximate the mode shape method. Then with the help of Rayleigh Ritz method we obtain the analytical value of frequencies. The analytical results are found to be closer to the experimental results with a maximum percentage error of about 15%. The model presented in the thesis can be extended to the mechanical structures with many non-uniform sections with or without bolted joints.

After the analytical modeling of bolted non-uniform beams with two and three sections, we did FEM modeling in ANSYS for the same. The effect of variation of torsional stiffness is studied along with the convergence of results. Importance is given to the modeling of joints in the FEM model with the use of coupling at the joint which equalises the degree of freedom for the both nodes being coupled. The results are found to be close to analytical and experimental results with minimal error.

Contents

Chapter 1

Introduction

Majority of mechanical and aerospace structures like missiles, aircrafts, [1], [2], submarines,etc are frequently modeled with the help of free-free Euler-Bernoulli beam. Euler Bernoulli beam theory is a simplification of the linear theory of elasticity which provides a means of calculating the load-carrying and deflection characteristics of beams. It covers the case for small deflections of a beam that is subjected to lateral loads only. It is thus a special case of Timoshenko beam theory. This theory can be used according to the boundary conditions of the structure such as free-free, fixed-free, etc. A majority of work focuses on the modal analysis of the tapered or non-uniform beam but study of a beam comprising of various varying cross sections beam connected by bolted joints which is the case in most of the important mechanical structures is very less. The inability of making seamless or monolithic mechanical and aerospace structures of large dimensions enforces a need to model jointed structures or the assembled structures. These structures have a complex boundary conditions at the joints and are critical with respect to vibrational analysis. The analysis of vibrational behaviour of the assembled structure at the joint is an important parameter to study for system designing.

1.1 Jointed sections

Majority of the mechanical structures are an assembly of various components or sections. They are joined together by means of different ways of fastening such as bolting, riveting, welding, extruding, clamping,gluing, etc. The location and the nature of the joints of a structure strongly influence the stiffness of the structure as well as the amount of damping and the occurrence of non linearities. Especially in structures made of metal,the amount of damping resulting from joints is typically higher than the material damping by a ten time to hundred times factor. The characterisation of joints based on the type of loading is done as normally loaded and tangentially loaded joints. In case of normally loaded joints the damping is very small compared to the tangentially loaded case. Main damping mechanisms are due to a phenomena known as 'gas-pumping' and local microscopic deformations of the asperities in the contact zone.This involves elastic and plastic deformation as well as microslip, especially if materials with different stiffness are in contact. Non-proportional and nonlinear softening effect in the structure is created as a result if joint gapping occurs and the resulting slapping or micro-impacts in the joint increase the influence of normal damping. For

joint connections under tangential load it should be differentiated between the occurrence of micro slip and macroslip. For tangential loading there is partial slip in the contact area while a larger part of the joint is still sticking. If the driving force becomes larger and/or the normal pressure decreases,at some instance the components begin to move relative to each other and macroslip occurs. In general,microslip and macroslip are nonlinear phenomena meaning that the superposition principle does not hold. However,experimental investigations often reveal a nearly linear behavior of the joints,as long as the excitation amplitudes are small and macroslip is avoided. Micro slip and macro slip are non linear phenomenon but in the case of jointed sections it is observed experimentally that in case of small amplitudes and macro slip, a linear behaviour is observed. For a jointed section subjected to periodic load, a hysteresis loop can be determined in the stress strain curve, which turns into elliptical shape if the case is that of sinusoidal load.

The jointed sections are classified as lumped models, line models and interface models depending on the dimensions of the model. In the case of the lumped model no spatial extension is considered if the joint size is small compared to the structure size. The contact area is also considered to be constant. The line models are 1-D models in which the contact area exhibits same properties in one direction while in interface models the phenomenon extends to 2-D.

1.1.1 Friction models

The friction force is a critical component of a joint. Based on the friction force the jointed models are classified as

- Quasi-Static Models

- Dynamic Models

- Hysteretic friction models

Quasi-static friction models

The Quasi-static models assume the frictional force to be static function of the relative velocity of joint surfaces. Dynamic models introduce more variables which change with respect to time. And the hysteretic models use dissipation energy and deformation criteria. The Coulomb model specifies a friction force in case of sliding and sticking should be treated separately. As an alternative to viscous model a constant hysteresis model can be used.It is based on the fact that many materials and joints show frequency/velocity- independent dissipation properties and depend solely on strain. An extension of the classical Coulomb model is introduction of stiction,which describes the friction force at rest. This force may be higher than Coulomb friction and it counteracts the motion of a structure until the initial displacement occurs.

Stribeck observed that the stiction force does not decreased is continuously, like in case with stiction,and defined a more complex nonlinear relation between the friction force and the sliding velocity. It is based on an observation that for low velocities the friction force continuously decreases and after reaching a certain minimum,called Stribeck friction,the force starts to increase again.

Jenkins element are the hysteresis curves for the Coulomb model and a combination of the Coulomb element with an elastic spring. The non-linear relationship between the force and displacement is shown from this curve, and the area enclosed corresponds to the dissipated friction energy.
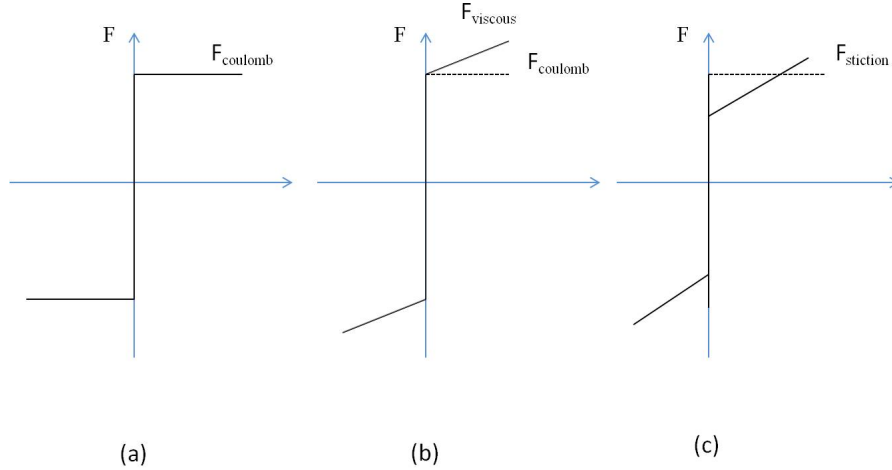
Figure 1.1: Quasi-static models(a)Basic Coulomb model (b)Coulomb model with viscous friction (c)Stiction with Coulomb model

The inability to describe the inelastic behaviour just before slip occurs at the joint necessitates for dynamic models.

Dynamic friction models

Fast and accurate friction models are required for control engineering which enforces the need to develop dynamic models. Dahl developed a dynamic friction model which is the generalization of Coulomb's model but with smooth transition around zero velocity. LuGre model further extends Dahl's model to reproduce additional friction phenomenon over wide range of operating conditions. Haessig and Friedland's model uses bristles for representing the two rough contact surfaces. A restoring force acts when the joint is subjected to tangential loading and the bristles deform. Leuven model is the extension of the LuGre model which aimed at improving the hysteretic behaviour in the microslip domain. Here the microslip behavior is substituted with hysteretic force function, with sliding regimes described by the same parameters as in the LuGre model.

Hysteretic friction models

These models take in account the elastic and plastic deformations at the joints along with the dissipative energies. Masing developed such kind of model which consisted of Jenkins elements in parallel. Masing's model can be generalized in two ways,

- Several Jenkins element with a spring

- Several springs with Coulomb element in series

The first model is generally called the Masing model while the second one is termed as Iwan model. The hysteresis curve for Masing model converges for an increasing number of Jenkins elements.Alternatively, the Masing model can be modified by smoothing of the signum function, used to describe switching of various friction elements, by approximating the signum with an exponential
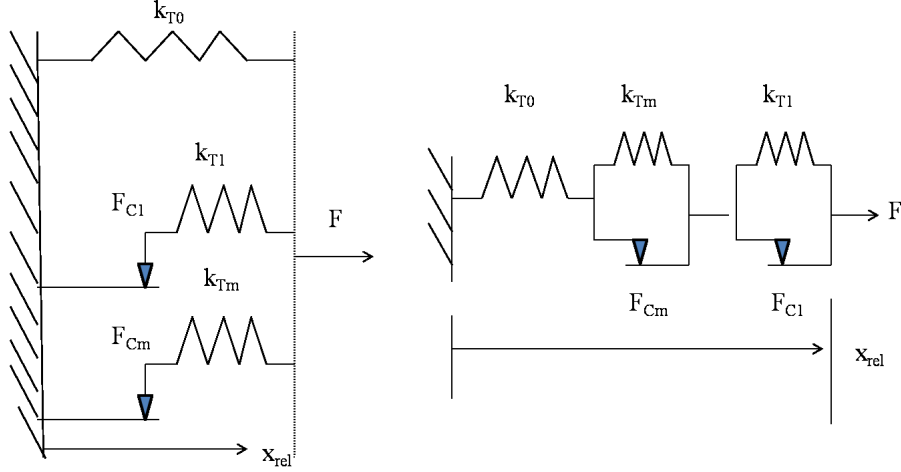
Figure 1.2: Hysteretic Friction models(a)Masing Model (b)Iwan Model

function Next model is the Bouc-Wen model which describes restoring force in system with hysteresis. It can be transformed into regularized Masing model and fit the measured hysteresis loops using certain parameters.

1.2 Literature review

Majority of mechanical and aerospace structures like missiles, aircrafts, submarines, etc., are frequently modeled as non-uniform free-free Euler-Bernoulli beam [1, 2, 3]. Although, there have been many work on the modal analysis of a structure with varying mass but there are limited studies available for a system of structures with varying cross sections which are connected by bolted joints. Since, most of important mechanical structures are the assembly of many sub structures, the analysis of non-uniform beams connected by bolted joint is very significant. In this paper, we deal with the modal analysis of single as well as bolted cantilever beams with non-uniform sections.

Abrate [4] studied the vibration of non-uniform rods for which he transformed the equation of motions into the wave equation and found out that the natural frequencies of non uniform rods fixed at both ends is same as that of uniform rods. Wu and Ho [5] obtained the natural frequencies and mode shapes corresponding to the longitudinal and torsional vibrations of a non-uniform ship hull with large hatch openings using the finite-element method. Platus [1] employed Lagrangian approach to study nonlinear aeroelastic stability of flexible missiles having non-uniform sections. Pourtakdoust and Assadian [6] studied the effect of thurst on the bending behaviour of non-uniform flexible missiles. Jaworski and Dowell [7] obtained the theoretical and experimental frequencies of a cantilever beam with multiple steps using the Rayleigh-Ritz method. Zheng et al. [8] developed modified vibration functions by satisfying the required boundary conditions to compute the frequencies of a multi-span beams with non-uniform sections subjected to moving loads.

However, none of the above studies assumed the joints as bolted joint. To model the jointed structure, there exist different types of models which are classified based on loading, damping, flexibility of the joints, etc [9]. While the normally loaded joint produces less damping as compared to tangentially loaded joint, the damping in tangentially loaded joint depends on its elastic and plastic deformation

due to micro- and macro-slip phenomena. Such behavior can be modeled using finely meshed finite element models or different friction models. Some of friction models are the Coulomb models, Masing model, Iwan model, etc. The nonlinear hysteretic behavior can be capture by different arrangements of Jenkin element, which is a combination of spring and friction slider, or the Bouc Wen model, etc. More details about the joint modeling can be found in reference [9, 10]. Oldfield et al. [11] used simplified models of bolted joints as a combination of the number of Jenkins elements and the Bouc-Wen model to study the effect of harmonic loading on a bolted joint using finite element method. Todd et al. [12] performed experiments on a beam with its boundaries supported by spring modified fasteners. Subsequently, they modeled the bolted joint with an effective spring stiffness based on the perpendicular load acting normal to the axis of the joint, i.e., neglecting the shearing effect, and thus, the effect of friction. Ouyang et al [13] conducted experiment on a single joint of two beams under torsional dynamic loads and described the hysteresis phenomena under different preloads and excitation amplitudes. Finally, they correlated the results with the micro and macro-slip phenomena at the joint interface. Ma et al [14] performed experiment on the bolted and unbolted structure. They found the nonlinear stiffness and damping associated the bolted joint by comparing the numerical model with the unbolted joint. Hartwigsen et al [15] performed experiment to characterize the non-linear effect of a shear lap joint on the dynamics of two mechanical structure. They modeled the effective stiffness and damping effect using Iwan models. Quinn [16] presented the modal analysis of jointed structures by modeling the elastic effect of the joint using a linear modal equation and the dissipative effect of the joint with a continuum series-series Iwan model. Tol and Özgüven [17] described an experimental identification method based on frequency response function decouling and optimization to extract the joint properties in terms of translation, rotational, and cross-coupling stiffness and damping values. Chen et al. [18] used the numerical assembly method (NAM) for computing the natural frequencies of a cantilever beam having multiple spans of different cross-sections carrying spring-mass system at different locations. In this method, they considered the joints as attaching points of two beams, and, then, used the equilibrium and compatibility equations to form element matrices to compute the natural frequencies. Song et al [19] presented the modeling of bolted beam structure using finite element method with adjusted Iwan beam elements obtained by taking two adjusted Iwan model corresponding to each degrees of freedom of 2-noded beam element. Subsequently, they used multi-layer feed forward neural network to optimize the joint parameters obtained from FEM model with the measured results. Eriten et al [20] ultilized nonlinear system identification and reduced order modeling to extract the nonlinear damping of beams with bolted joints. They have also compared the results with monolithic structure. Ahmadian and Jalali [21] presented a nonlinear parametric formulation through a generic element under the conditions of a joint interface. They obtained the dynamic characteristics of joint by comparing the dynamic response of generic element using the incremental harmonic balance with the observed behavior of the structure. To do accurate nonlinear friction modeling of the jointed structure for general structure, Süß and Willner [22] first used three degree-of-freedom model using Multiharmonic Balance Method (MHBM) and then extended it to n degrees-of-freedom model using the finite element method. Since the accuracy of harmonic balance method increases with the number of harmonics, increase in harmonics leads to larger computation time. To reduce the computation time, Jaumouillé et al [23] proposed an adjusted harmonic balance method which adjusts the number of retained harmonics for a given precision and frequency value. Although there have been many

improvement in the modeling of bolted structures, however, some level of uncertainties remains due to non-smooth nonlinear dynamic characteristics [24]. It is also important to note that most of the above literatures dealt with the bolted joint of only uniform beams. To do the modeling of jointed beams with non-uniform beams, Sarkar and Ganguli, [25], adopted an inverse problem approach to obtain fundamental mode shape of a single as well as bolted non-uniform Euler Bernoulli beams by approximating the variation of mass and flexural rigidity by polynomial of required order in conjunction with free-free Euler-Bernoulli beam. To do the analysis of bolted non-uniform beam, they modeled the bolted joint with torsional spring. However, their analysis is limited to the first mode of free-free non-uniform beam.

In this thesis, we focus on the modal analysis of jointed cantilever beams with non-uniform sections using higher modes. To do the analysis, we first compute the mode shapes and frequencies of
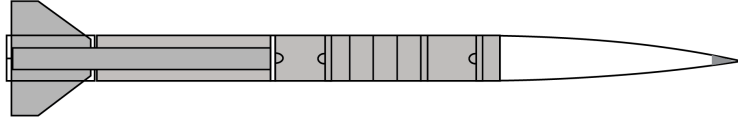
Figure 1.3: Application of non-uniform beam

first three modes of a non-uniform cantilever beam using experimental and numerical analysis. Subsequently, we follow the approach proposed by Sarkar and Ganguli [25] to theoretically compute the mode shapes and frequencies, and then, compare them with the experimental and numerical results. To characterize the bolted joint, we use the same approach to model the system of bolted non-uniform beams with two and three sections, separately. Finally, we compare the results with the experimental as well as numerical values.

1.3 Outline of thesis

This thesis is divided into five chapters. In the first chapter we introduce the topic of our study. The chapter presents the previous works done in the corresponding field and the approach that we follow. Various literature dealing with non-uniform beam is studied along with the literature on jointed structures. The chapter also presents the type of modal analysis approached that can be adopted for the vibrational analysis of non-uniform bolted beams. The second chapter presents the frequency analysis of a simply supported cantilever beam. The study is conducted on single non-uniform beams and continued for bolted three section beams. The dimensions are taken as mentioned by Sarkar and Ganguli, [25]. The frequency analysis is done analytically and numerically for the first three modes. Different types of non-uniform beams based on the variation of stiffness and mass are studied. The use of approximate mode shape method for the modal analysis of bolted beams is introduced for the higher modes. In the next chapter the approach adopted in the second chapter is extended to a beam which is treated as a cantilever beam. This chapter presents the work which is based on the mechanical structures in fixed free configuration. Single non-uniform beams are studied and then the study is extended to two section and three section bolted beams. Also to find the effect of bolted joints on structure, a monolithic beams consisting of no bolts is studied analytically and experimentally. First step is the experimental procedure conducted on vibrometer and then the results are validated with the help of analytical and numerical model. The

analytical modeling is done with the help of approximate mode shape expressions based on the approach adopted by Sarkar and Ganguli,[25]. The fourth chapter presents the numerical analysis of bolted beam with two and three sections. This chapter presents the numerical analysis of only bolted structures. The use of coupling element is is presented and different cases are studied. The effect of bolted stiffness is studied for the beams. The last chapter concludes the work and suggests the future work that can be done. The limitations and the scope to which this work can be extended is discussed.

Chapter 2

Frequency analysis of non-uniform simply supported beams

In this section, we present systematic approach to compute the mode shape of a non-uniform beam with variable mass and elastic rigidity by following the approach for first mode as mentioned by Sarkar and Ganguly,[25]. In this chapter,we assume a prescribed polynomial,as the fundamental mode shape which satisfies the boundary conditions of a non-uniform freefree beam.Then we have used the inverse problem approach to show that for certain mass and stiffness distributions of the beam,there exists a simple closed-form solution given by the assumed polynomial. Subsequently, we compare the mode with the numerical solution obtained from ANSYS. Later, we extend the method to compute the second and third modes of a single non-uniform beam, and to the second mode of bolted non-uniform beam system. Finally, we also compute the frequencies using the obtained mode shapes of a single beam as well as bolted beam systems, respectively, and compare the results with numerical results from ANSYS. The proposed approach also allows us to design freefree beams with tailored mode shapes and specified nodal locations.

2.1   Mode shape computation

In this section, we compute the mode shapes of a single non-uniform beam for the first three modes and then extend the theory to compute the first two modes of a bolted system of three non-uniform beams. The approach followed is the approximate mode shape approach where we assume the mode shape as polynomial expression and used the boundary conditions of a free-free beam to find out the variables in the expression. Also the variations of mass and stiffness is takes as polynomial expressions and is obtained after the mode shape is calculated. For the higher modes we use the zero location boundary conditions observed from the numerical analysis. For the bolted joint beam we use the torsional spring boundary condition as to take care of the moment being transferred at the joint. No damping is considered in our case.

2.1.1 Single non-uniform beam

A non-uniform beam of length L, width W, thickness H, mass m, elastic modulus E, area moment of inertia I, etc., can have varying section along its length based on a variation having inclined line with zero curvature, concave curve with negative curvature and a convex curve with positive curvature as shown in Figure 2.1. Based on the type of non-uniformity, the zero position of the higher order modes change to different location. To demonstrate such variation, we take a non-uniform beam with linearly varying section in this paper. We first validate the approach with that obtained by Sarkar and Ganguli, [25], and then extend the theory to the second and third modes, respectively. The mathematical formulation of a single non-uniform free-free beam can be modeled by the Euler
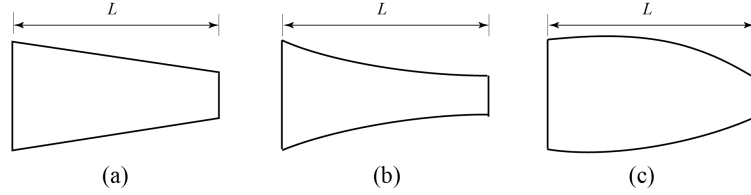
Figure 2.1: A single non-uniform beam with the side curve having curvature of (a) zero, (b) negative, and (c) positive, respectively.

Bernoulli beam equation. The modal analysis can be done with the help of assumption of mode shapes satisfying the respective boundary conditions for the modes. Taking the same variation of mass per unit length, m(x), and the flexural rigidity, EI(x), due to non-uniform variation of section of the beam along its length as mentioned by Sarkar and Ganguli, [25], we get

$$m(x) = a_0 + a_1 x \tag{2.1}$$

$$EI(x) = b_0 + b_1 x + b_2 x^2 + b_3 x^3 + b_4 x^4 + b_5 x^5 \tag{2.2}$$

where, $a_i s$, and $b_i s$ are constant coefficients.

First mode

Taking the assumed mode shape (x) for the first mode as

$$\phi(x) = c_0 + c_1 x + c_2 x^2 + c_3 x^3 + c_4 x^4 + c_5 x^5 + c_6 x^6 \tag{2.3}$$

where, the coefficients $c_0, c_1, c_2, c_3, c_4, c_5, c_6$ are obtained based on the boundary conditions corresponding to free-free simply supported beam and normalization condition. The order of polynomial expression used for mode shape depends on the boundary condition that are to be satisfied by the concerned mode shape. The use of exact mode shape is restricted as it's adoption will not be helpful in capturing all the boundary conditions. The order of the polynomial mode shape used by us is flexible and hence can be increased or decreased depending on the boundary conditions. Since the free-free simply supported beam has two zero locations corresponding to its first mode, we obtain the above coefficients associated with $\phi(x)$ in terms of α and β, where, α and β represent the two zero locations from origin O . Approximating the displacement by a single mode, Euler Bernoulli

equation can be written as,

$$\frac{\partial^2}{\partial x^2}\left(EI(x)\frac{\partial^2 \phi}{\partial x^2}\right) - m(x)\omega^2 \phi(x) = 0 \tag{2.4}$$

where, ω denote the first modal frequency. Substituting the expressions of $m(x), EI(x)$, and $\phi(x)$ in equation 2.4, and then comparing the coefficients of different powers of x, we obtain a set of algebraic equation in terms of $\alpha, \beta, a_0, a_1, b_0, b_1, b_2, b_3, b_4, b_5, b_6$. Taking X = $[a_0; a_1; b_0; b_1; b_2; b_3; b_4; b_5; b_6]$, algebraic equation can be written in the form of a matrix, $AX = 0$. For a non-trivial solution, we set the determinant of the matrix A to zero, and, obtain the characteristics equation in terms of α and β. By setting one of the value of zero location of the beam with length L=5 m, say, $\alpha = 0.78L$=3.9, we obtain β=0.226L= 1.13. The results are found to be same as that obtained by Sarkar and Ganguli [25]. Finally, the analytical mode shape corresponding to the first mode is obtained as

$$\phi(x) = 1.05 - 0.96\,x + 0.038\,x^4 - 0.009\,x^5 + 0.0006\,x^6 \tag{2.5}$$

To compare the validity of the mode shape, we also did modeling in ANSYS. For the modeling, we take a non-uniform beam of elastic modulus, $E = 200GPa$, and $\rho, = 7840kg/m^3$ with a length of L=5 m. At x=0, we take the width W=0.0560 m and thickness H=0.00428 m, and at $x = L$, the width and thickness are taken as W=0.05413 m and H=0.00443 m. Subsequently, we do modal analysis to find the frequencies and the corresponding mode shapes. On comparing the zero positions obtained numerically from ANSYS with the analytical results from equation 2.5 as shown in Table 2.1 and Figure 2.2 , we found a good match with a percentage error of about 2%. Thus, our analytical and numerical models are now validated. In the subsequent sections, we extend the analytical and numerical modeling to obtain the mode shapes of second and third modes.

Second mode

Using the numerical solution in ANSYS as described in the previous section, we also obtain the mode shapes of second and third modes. Using the second mode shape as obtained in Figure 2.1, we noticed that there are three zero positions in the second mode. Therefore, it requires additional boundary condition as compared to the case of first mode. Consequently, the order of the assumed polynomial for the second mode shape is increased by one in order to satisfy additional zero position boundary condition. Therefore, the assumed mode shape can be written as

$$\phi(x) = c_0 + c_1 x + c_2 x^2 + c_3 x^3 + c_4 x^4 + c_5 x^5 + c_6 x^6 + c_7 x^7 \tag{2.6}$$

The corresponding boundary conditions can be written as,

$$\phi''(0) = 0, \phi'''(0) = 0, \phi''(L) = 0, \phi'''(L) = 0, \phi(\alpha) = 0, \phi(\beta) = 0, \phi(\gamma) = 0, \phi(L) = -1, \tag{2.7}$$

Using the boundary conditions given by eqn. (7), cis can be written in terms of zero position α, β , andγ. Substituting the expressions of $m(x), EI(x)$, and $\phi(x)$ in eqn. (4), and then comparing the coefficients of different powers of x, we obtain a set of algebraic equation in terms of α, β,γ ,$a_0, a_1, b_0, b_1, b_2, b_3, b_4, b_5, b_6$. Taking X = $[a_0; a_1; b_0; b_1; b_2; b_3; b_4; b_5; b_6]$, the algebraic equation can be written in the form of a matrix, AX=0. For a non-trivial solution, we set the determinant of the

matrix A to zero, and, obtain the characteristics equation in terms of α, β and γ. Taking the values of $\alpha = 0.22L{=}1.1$ and $\beta{=}0.78L{=}3.9$ based on the numerical mode shape, we obtain $\gamma = 0.52L{=}2.6$. On comparing it with the numerically obtained values in Table 1 and Figures 3(b) and (e), we found a percentage difference of about 4%. The analytical form of the second mode can be written as,

$$\phi(x) = 1.12 - 1.16\,x + 0.19\,x^4 - 0.09\,x^5 + 0.01\,x^6 - 0.0008\,x^7 \tag{2.8}$$
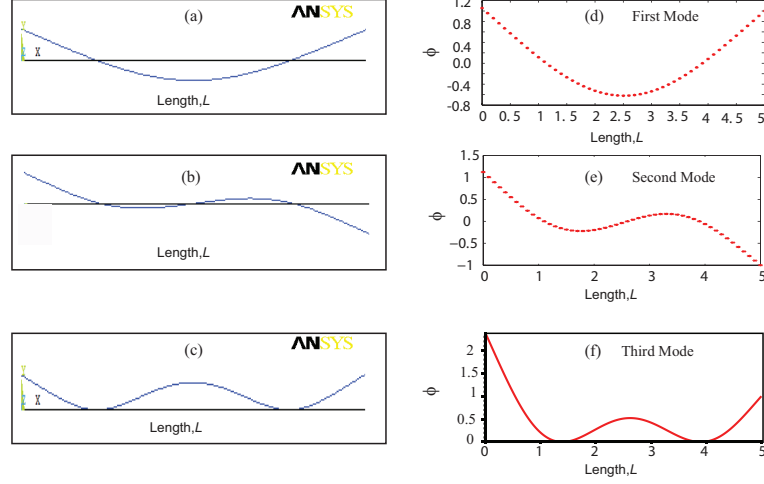
Figure 2.2: Comparison of three mode shapes of a non-uniform beam obtained from numerical and analytical methods, respectively.

Third mode

Like the case of second mode, we first obtain the mode shape corresponding to the third mode as shown in Figure2.2(c). Based on numerically obtained mode shape, we found in addition to two zero locations, the slopes at these locations are also zero. To capture the additional effects, we assume the third mode shape as a polynomial of order eight as follows,

$$\phi(x) = c_0 + c_1x + c_2x^2 + c_3x^3 + c_4x^4 + c_5x^5 + c_6x^6 + c_7x^7 + c_8x^8 \tag{2.9}$$

The corresponding boundary conditions can be written as,

$$\phi''(0) = 0, \phi'''(0) = 0, \phi''(L) = 0, \phi'''(L) = 0, \phi(\alpha) = 0, \phi(\beta) = 0, \phi'(\alpha) = 0, \phi'(\beta) = 0, \phi(L) = 1 \tag{2.10}$$

Following the similar approach as in the case of first and second mode, we obtain $AX{=}0$, where, X = $[a_0; a_1; b_0; b_1; b_2; b_3; b_4; b_5; b_6]$. To obtain the non-trivial solution, we set the determinant of the matrix A to zero, and, obtain the characteristics equation in terms of α, and β. Taking $\beta{=}0.78L{=}3.90$, we analytically obtain $\alpha{=} 0.278L{=}1.39$, which is in close approximation of $0.28L$ as achieved in ANSYS. Substituting the above $\phi(x)$ in the governing equation and solving the set of equations in matrix form, i.e. keeping the determinant of A=0 for the non trivial solution we get an equation in terms of α and ϕ. On providing the value of $\beta{=}0.78L$, we achieved the value of $\alpha{=} 0.278L{=}1.39$, which is in close agreement with numerically computed values of $0.28L{=}1.4$ as obtained using ANSYS. Finally,

the approximate expression of third mode can be written as,

$$\phi(x) = 2.36 - 2.68\,x + 1.13\,x^4 - 0.83\,x^5 + 0.23\,x^6 - 0.03\,x^7 + 0.001\,x^8 \tag{2.11}$$

Table 2.1: Frequency comparison for Single non-uniform beam

Mode Parameters	Mode 1		Mode 2			Mode 3	
	α	β	α	α	γ	α	β
Theoritical	1.13	3.90	1.10	3.90	2.60	1.39	3.90
Numerical	1.10	3.90	1.10	3.90	2.50	1.4	3.90

The zero positions of the third mode obtained analytically and numerically are mentioned in Table 2.1

2.1.2   Non-uniform beams with bolted joints

In this section, we apply the approach described in the previous section to obtain first and second mode shape of bolted non-uniform beams as shown in Figure 4. To do the analysis, we take the same dimensions as mentioned by Sarkar and Ganguli [25], who have done the similar analysis for the first mode. In this section, we validate the modeling of bolted non-uniform beams with numerical solution from ANSYS. To do the modeling, we take three non-uniform beams of elastic modulus, $E = 200GPa$, and ρ, $= 7840kg/m^3$ with a length of L_1=1.1 m, L_2=2.8m and L_3=1.1m such that $L = L_1 + L_2 + L_3$=5 m. The width and height of initial and final sections of each beam are mentioned in Table 2. The coupling of the beams which are bolted between the first and second beams and the second and third beams are provided by coupling element COMBIN14. To induce the coupling at the joint, we take the stiffness value of 100 Nm/rad at the junction of first and second beams and 150 Nm/rad at the junction of second and third beams. Finally, based on the modal analysis, we obtain the first two modes of the bolted non-uniform beam as shown in Figures 5(a) and (c). In the following sections, we compute the mode shape of bolted beams corresponding to first and second mode using the information from numerically obtained mode shapes.
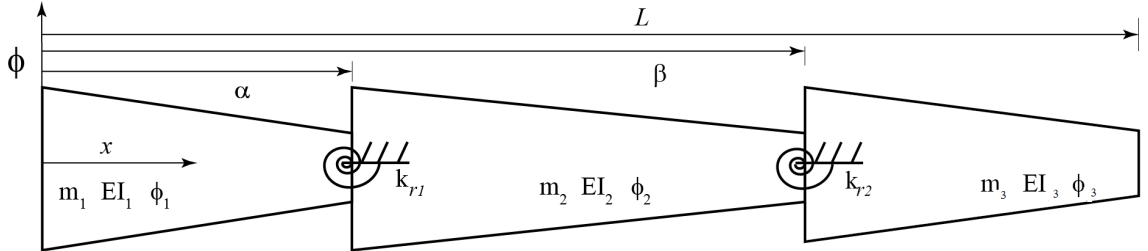

Figure 2.3: Schematic diagram of considered bolted beam

Table 2.2: Width and height of three non-uniform beams bolted together

Non-Uniform Beam	Length [m]	Initial Cross Section [m]	Final Cross Section [m]
Beam 1	L_1=1.1	H=0.0059 W=0.0159	H=0.006802 W=0.01522
Beam 2	L_2=2.8	H=0.003596 W=0.25795	H=0.003679 W=0.2409
Beam 3	L_3=1.1	H=0.004722 W=0.17095	H=0.005239 W=0.12515

First mode

In this section, to analytically compute the first mode of a free-free bolted non-uniform beam, we follow the same approach as proposed by Sarkar and Ganguli [25]. Based on the numerically obtained mode shape as shown in Figure 2.4, it is noted that the zero positions are located at the intersection of different beams. The boundary conditions are formulated with the help of the information obtained from the numerical model. To obtain the complete mode, the mode shape of individual beams are taken separately. Again the order of the polynomial depends on the boundary condition needed to be satisfied by the mode shape. In this case as the second mode shape or the mode shape for the second section needs to satisfy one extra boundary condition which is common to both the sections, hence the order of the second section mode shape is chosen as one higher than other two.

$$\phi_1(x) = a_0 + \frac{a_1 x}{L} + \frac{a_2 x^2}{L^2} + \frac{a_3 x^3}{L^3} + \frac{a_4 x^4}{L^4} + \frac{a_5 x^5}{L^5}$$
$$\phi_2(x) = b_0 + \frac{b_1 x}{L} + \frac{b_2 x^2}{L^2} + \frac{b_3 x^3}{L^3} + \frac{b_4 x^4}{L^4} + \frac{b_5 x^5}{L^5} + \frac{b_6 x^6}{L^6}$$
$$\phi_3(x) = c_0 + \frac{c_1 x}{L} + \frac{c_2 x^2}{L^2} + \frac{c_3 x^3}{L^3} + \frac{c_4 x^4}{L^4} + \frac{c_5 x^5}{L^5} \tag{2.12}$$

Corresponding to the free-free boundary conditions and continuity conditions in the displacement, slope, shear force and bending moment at the joints located at x= α and β, we get the following conditions,

$$\phi_1''(0) = 0, \phi_1'''(0) = 0, \phi_3''(L) = 0, \phi_3'''(L) = 0, \phi_1(\alpha) = 0, \phi_2(\alpha) = 0, \phi_2(k) = 0, \phi_3(\beta) = 0,$$
$$\phi_2(\beta) = 0, \phi_3(L) = -1, EI_1 \frac{d^2}{dx^2}\phi_1(\alpha) = -k_{r1}\frac{d}{dx}\phi_1(\alpha) + EI_2\frac{d^2}{dx^2}\phi_2(\alpha) \, EI_2\frac{d^2}{dx^2}\phi_2(\beta)$$
$$= -k_{r2}\frac{d}{dx}\phi_2(\beta) + EI_3\frac{d^2}{dx^2}\phi_3(\beta) \, EI_1\frac{d^3}{dx^3}\phi_1(\alpha) = EI_2\frac{d^3}{dx^3}\phi_2(\alpha), EI_2\frac{d^3}{dx^3}\phi_2(\beta)$$
$$= EI_3\frac{d^3}{dx^3}\phi_3(\beta) \, \frac{d}{dx}\phi_1(\alpha) = \frac{d}{dx}\phi_2(\alpha), \frac{d}{dx}\phi_2(\beta) = \frac{d}{dx}\phi_3(\beta) \tag{2.13}$$

Finally, satisfying the governing equation at the joints corresponding to x= α and β, such that $EI_i\phi_i''''(x) = m_i(x)\omega^2\phi_i(x)$, we get $\phi_1''''(\alpha) = 0, \phi_2''''(\alpha) = 0$ and $\phi_2''''(\beta) = 0 \, and \, \phi_3''''(\beta) = 0$. Solving the above equations normalizing it at x=L, we obtain the unknown coefficients of the individual

modes of the beams corresponding to the first mode. Finally, we get,

$$\phi_1(x) = 2.48 - 1.39\,x + 0.019\,x^4 - 0.0019\,x^5$$
$$\phi_2(x) = 2.91 - 2.96\,x + 2.11\,x^2 - 1.37\,x^3 + 0.46\,x^4 - 0.0721\,x^5 + 0.004\,x^6$$
$$\phi_3(x) = -4.28 + 9.98\,x - 7.14\,x^2 + 2.14\,x^3 - 0.28\,x^4 + 0.014\,x^5 \qquad (2.14)$$

Second mode

To find the analytical expression of the second mode of a system of bolted non-uniform beams, we first obtain the numerical mode shape in ANSYS as shown in Figure 2.4. It shows that there is an additional zero position in the middle beam and the displacement of the free ends are in the opposite directions. While the additional zero in the middle beam, say at $x = k$, can be captured by increasing the order of the assumed mode by one, the displacement of the last beam at the free end is captured by normalizing its mode shape with respect to -1. Taking the mode shapes of first, second and third beams as,

$$\phi_1(x) = a_0 + \frac{a_1 x}{L} + \frac{a_2 x^2}{L^2} + \frac{a_3 x^3}{L^3} + \frac{a_4 x^4}{L^4} + \frac{a_5 x^5}{L^5}$$
$$\phi_2(x) = b_0 + \frac{b_1 x}{L} + \frac{b_2 x^2}{L^2} + \frac{b_3 x^3}{L^3} + \frac{b_4 x^4}{L^4} + \frac{b_5 x^5}{L^5} + \frac{b_6 x^6}{L^6} + \frac{b_7 x^7}{L^7}$$
$$\phi_3(x) = c_0 + \frac{c_1 x}{L} + \frac{c_2 x^2}{L^2} + \frac{c_3 x^3}{L^3} + \frac{c_4 x^4}{L^4} + \frac{c_5 x^5}{L^5} \qquad (2.15)$$

and the boundary conditions can be written as,

$$\phi_1''(0) = 0, \phi_1'''(0) = 0, \phi_3''(L) = 0, \phi_3'''(L) = 0, \phi_1(\alpha) = 0, \phi_2(\alpha) = 0, \phi_2(k) = 0, \phi_3(\beta) = 0, \phi_2(\beta) = 0,$$

$$\phi_3(L) = -1, EI_1 \frac{d^2}{dx^2}\phi_1(\alpha) = -k_{r1}\frac{d}{dx}\phi_1(\alpha) + EI_2\frac{d^2}{dx^2}\phi_2(\alpha)\,EI_2\frac{d^2}{dx^2}\phi_2(\beta) = -k_{r2}\frac{d}{dx}\phi_2(\beta)$$

$$+ EI_3\frac{d^2}{dx^2}\phi_3(\beta)\,EI_1\frac{d^3}{dx^3}\phi_1(\alpha) = EI_2\frac{d^3}{dx^3}\phi_2(\alpha), EI_2\frac{d^3}{dx^3}\phi_2(\beta) = EI_3\frac{d^3}{dx^3}\phi_3(\beta)\,\frac{d}{dx}\phi_1(\alpha)$$

$$= \frac{d}{dx}\phi_2(\alpha), \frac{d}{dx}\phi_2(\beta) = \frac{d}{dx}\phi_3(\beta) \qquad (2.16)$$

Like the case of first mode, the assumed modes satisfying the governing equations at the joints will lead to $\phi_1''''(\alpha) = 0, \phi_2''''(\alpha) = 0$ and $\phi_2''''(\beta) = 0 and \phi_3''''(\beta) = 0$. Normalizing the mode of the third beam at the free end such that $\phi_3(L)$=-1 , we obtain the following form of the mode shape,

$$\phi_1(x) = 3.54 - 3.44\,x + 0.16\,x^4 + 0.003\,x^5$$
$$\phi_2(x) = -1.63 + 17.63\,x - 33.23\,x^2 + 25.89\,x^3 - 10.46\,x^4 + 2.34\,x^5 - 0.27\,x^6 + 0.013\,x^7$$
$$\phi_3(x) = -77.18 + 78.36\,x - 31.06\,x^2 + 6.08\,x^3 - 0.59\,x^4 + 0.02\,x^5 \qquad (2.17)$$

2.2 Frequency analysis

In this section, we utilize the mode shape computed in the previous section to compute the modal frequencies of single as well as bolted non-uniform beams. The Rayleigh Ritz method has the advantage that instead of discretization by dividing into elements we can discretize by assuming
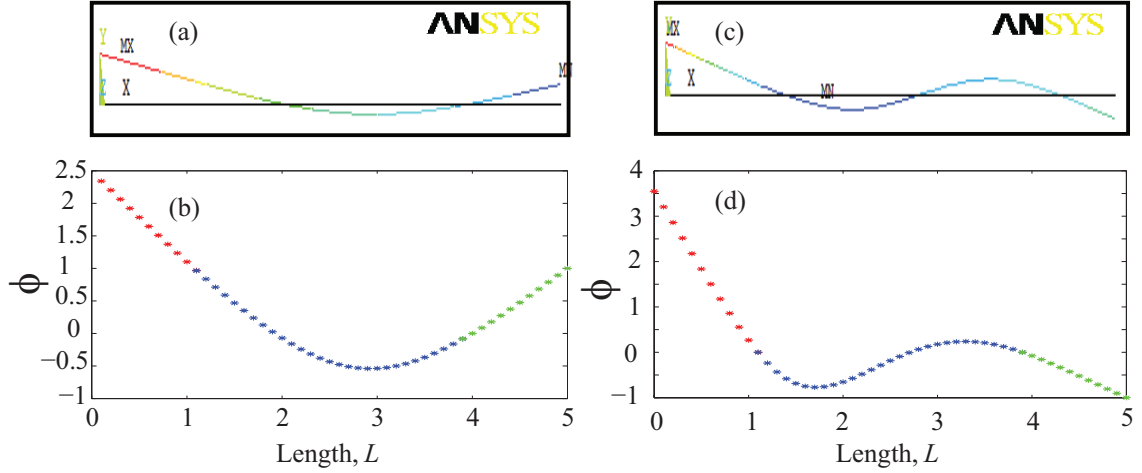
Figure 2.4: Modes of three non-uniform bolted beams obtained in ANSYS and MAPLE

solution in form of series. The method uses a series of assumed functions that satisfies kinematic boundary condition and find coefficients by minimizing Rayleigh quotient.

$$\omega_n^2 = \frac{\sum \int_0^L \frac{\partial^2}{\partial x^2} \left(EI(x)_i \frac{\partial^2 \phi_i(x)}{\partial x^2} \right) \phi_i(x)}{\sum \int_0^L m(x)_i \phi_i^2(x) dx} \tag{2.18}$$

where,ω is the nth angular frequency and $f_n = \frac{\omega_n}{2\pi}$ is the corresponding frequency in Hz, i denotes ith beam. Table 2.3 shows the comparison of frequencies of single non-uniform beam and bolted beams computed by analytical method and that from the numerical simulation in ANSYS.

Table 2.3: Frequencies of single non-uniform beam and three non-uniform bolted beams

Mode Number	Single Non-Uniform Beam		Three Non-Uniform Bolted Beams	
	FEM[Hz}	Analytical[Hz]	FEM[Hz]	Analytical[Hz]
First Mode	0.90	0.85	1.24	1.23
Second Mode	1.73	1.61	3.11	2.66
Third Mode	2.90	2.227	-	-

2.3   Summary and result discussion

In this section we presented the mode shape and frequencies of single non-uniform and bolted cantilever beams. We start our work with mode shape computation for non-uniform single beams analytically and numerically. The study is then is extended to the analytical model of bolted joints sections with simply supported configuration. The study is extended to the higher vibrational modes. On comparing the results with the numerical model we find reasonable match, thus proving closed form solutions to be effective while studying vibration in non-uniform beams.

With the results as shown in Table 2.3 it can be seen that the analytically obtained frequency values are less than the numerically obtained values. The reason for this can be accounted by the fact that we use approximated mode shape approach for the analytical model instead of exact mode shape approach. The use of this approach might be useful for some practical design applications where

the fundamental frequency might be required to assume a desired value or if the location of the internal nodes needs to be shifted. At the bolted section,the external elastic constraints are present, where we consider two rotational constraints at the internal nodes,and consequently divided the beam into three sections having variable mass and stiffness per unit lengths. We assumed simple polynomial mode shapes for each of the three sections and derived them using all the relevant boundary conditions of the non-uniform freefree beam, which leads to another class of closed-form solutions and also enables us to tailor the internal node locations, given a certain fundamental frequency and other beam parameters.

Chapter 3

Frequency analysis of non-uniform cantilever beam

This chapter extends the study done in previous chapter on simply supported configuration to beams with cantilever configuration. This configuration is of critical importance for the mechanical structures that is fixed to the ground with the other end free. The approach followed is same of approximate mode shape analytical model. The study also presents the experimental procedure conducted on the beam. The result for the same are verified with the analytical and numerical models. First three vibrational modes are analysed for all the cases.

3.1   Experimental procedure

To measure the modal frequencies of single as well as bolted non-uniform beams as shown in Fig. 3.1(b), we use Polytec scanning laser vibrometer as described in Fig. 3.1(a). To perform the experiment, we first mount the test specimen on a shaker. Subsequently, we apply pseudorandom signal from an internal function generator of vibrometer over a frequency bandwidth of around 200 Hz to 1600 Hz so as to cover the first three transverse modes of different configurations. In each case, the FFT lines are taken as 3200 over the given bandwidth. The acceleration of shaker is controlled through the amplifier. To capture the mode shape and modal frequencies, we defined scanning points on the test sample using laser scanning head and start the measurements of displacement/velocity at each points of the defined region. The movement of laser over the scan points are controlled using OFV controller. Finally, the measured quantities such as the displacement or velocity and input signal are stored using data acquisition system over a given frequency range. The accuracy of frequency measurements depends on the number of FFT lines and frequency bandwidth. A detailed description of measurement technique is described in the references [14, 26, 27].

3.2   Fixture design

The specimen on which the experiment is conducted are fixed on a fixture that is mounted on the top of the shaker. As the fixture acts as the medium to transfer the vibration from the shaker to the specimen, hence it is important to study the vibrational behaviour of the fixture. Therefore an
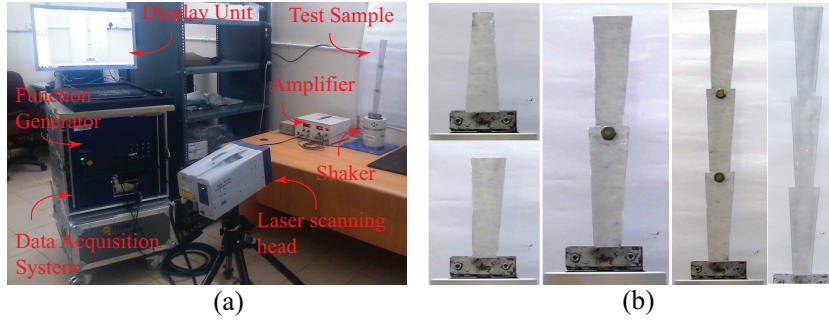
Figure 3.1: (a) A picture showing the outline of experimental setup; (b) Test specimen showing the images of single non-uniform beam, bolted beams with two and three non-uniform sections, and a monolithic beam with three non-uniform sections without bolted joint.

experiment was conducted in which the frequency response of the fixture was acquired and analysed. The fixture setup is shown as in figure 3.3.

For the experimental procedure a pseudorandom signal is used as an input. The bandwidth for the procedure was ranging from 0 Hz to 4 KHz to capture all the behaviour. The FFT lines taken are 3200. The frequency vs response graph obtained is as shown in Figure 3.4

- The frequency response curve obtained peak at 183.75 Hz which is a noise and no significant mode. The next frequency at which peak was obtained is 878.75 Hz which is the first torsional mode. The second torsional mode is obtained at 995 Hz. The first clear transverse mode is obtained at 2063.25 Hz. From the frequencies obtained we can conclude that the effect of fixture will be significant for the single non-uniform beams where the third mode is obtained close to 1000 Hz. And it will have less significance for the bolted beams.

The experimental setup consisted of a PSV-500 Scanning Vibrometer, a Polytec product for optical non-contact vibration mapping and analysis.The main components of a PSV-500 Scanning vibrometer are PSV-I-500 Scanning Head with high precision scanner and HD video 20x zoom camera PSV-F-500 Front-End with digital broadband decoder. It also comprises of PSV-W-500-M Data Management System: 19 industrial PC with data acquisition and signal generator board.At the heart of every Polytec vibrometer system is the laser-Doppler vibrometer a precision optical transducer used for determining vibration velocity and displacement at a fixed point. The technology is based on the Doppler-effect; sensing the frequency shift of back scattered light from a moving surface. The working principle involves the Doppler effect in which a wave is reflected by a moving object and detected by a measurement system (as is the case with the LDV), the measured frequency shift of the wave can be described as

$$f = 2v/\lambda \tag{3.1}$$

where, v is the object's velocity and λ is the emitted wavelength. To be able to determine the velocity of an object, the (Doppler-)frequency shift has to be measured at a known wavelength. This is done in the LDV by using a laser interferometer. The Laser-Doppler vibrometer works on the basis of optical interference, requiring two coherent light beams, with their respective light intensities I1 and I2, to overlap. The resulting intensity is not just the sum of the single intensities. This interference term relates to the path length difference between both beams. If this difference
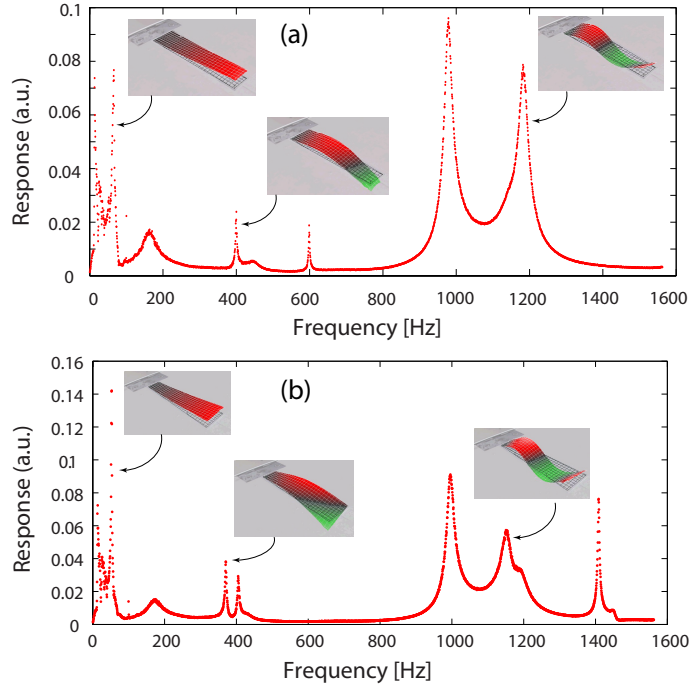
Figure 3.2: Experimental frequency response of a single non-uniform beam with (a) diverging section and (b) converging section.

is an integer multiple of the laser wavelength, the overall intensity is four times a single intensity. Correspondingly, the overall intensity is zero if the two beams have a path length difference of half of one wavelength.

The beam of a helium neon laser is split by a beam splitter (BS 1) into a reference beam and a measurement beam. After passing through a second beam splitter (BS 2), the measurement beam is focused onto the object under investigation, which reflects it. This reflected beam is now deflected downwards by BS 2 (see figure), is then merged with the reference beam by the third beam splitter (BS 3) and is then directed onto the detector.

Using the above mentioned procedure, we perform experiments to find the modal frequencies and mode shapes of single as well as bolted non-uniform beams as shown in Fig. 3.1. All the beams are made of aluminium and are of length, $L = 0.16$ m, thickness, $t = 0.002$m and have varying width of $b_1 = 0.03$ m at one end to $b_1 = 0.05$ m at another end. Each beam is provided with end holes of diameter $d = 0.01$ m and an extra length of 0.02 m is provided for the fastening. The Young's modulus and the density of aluminium beam are taken as $E = 69$ GPa and $\rho = 2700$ kg/m^3. The bolts used are of 0.01 m and one bolt is used for each jointed section.

Table 3.1: Experimental results for single and bolted non-uniform cantilever beams.

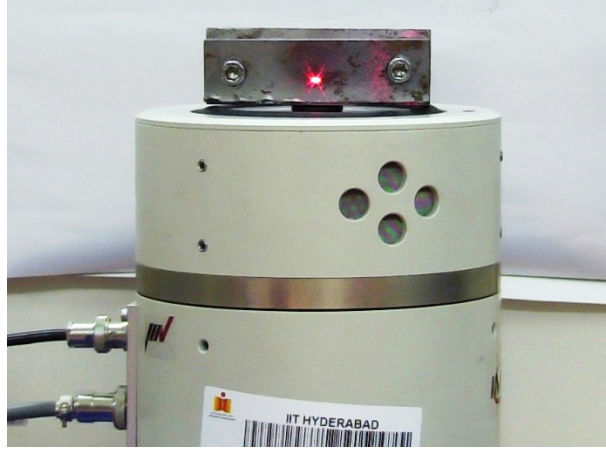| FEA models	1st mode	2nd mode	3rd mode
Single beam(Small end fixed)	54.68	371.09	1146.48
Single beam(Bigger end fixed)	66.40	401.36	1160.15
Two section bolted beam	13.1	66.5	260.25
Three sections monolithic beam	6.75	43.50	118.0
Three sections bolted beam	5.625	33.43	73.44

Figure 3.3: Experimental setup for fixture
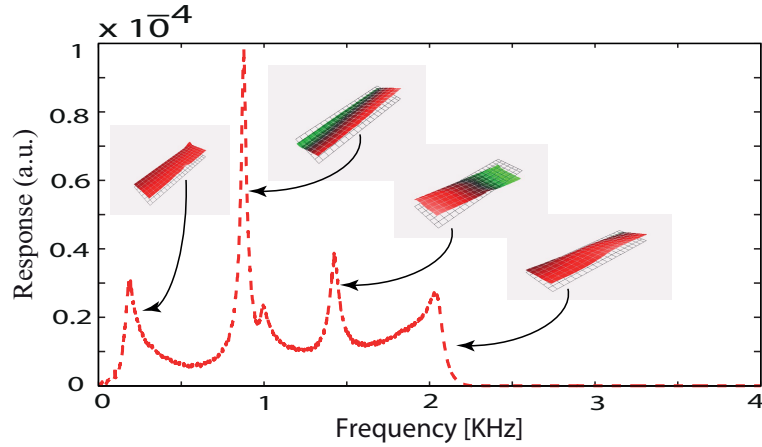
Figure 3.4: Frequency vs response curve obtained for fixture

To systematically perform the experimental studies, we first perform experiments on a single non-uniform cantilever beam. Figures 3.2(a) and (b) show the frequency response of the single non-uniform cantilever beam when its wider and smaller ends are fixed, respectively, as shown in Fig. 3.1(b). For the beam having fixed wider end, the first three transverse modes are found at 54.68 Hz, 371.09 Hz, and 1146.48 Hz. For the beam with smaller end fixed, the corresponding frequencies are found as 66.40 Hz, 401.36 Hz, and 1160.15 Hz. Based on the observation of second mode, it is found that the first torsional and second transverse modes are closer to each other. Figure 3.5 show the variation of frequency response of a bolted cantilever beam with two non-uniform sections. The frequencies are found to be 13.1 Hz 66.5 Hz, and 260.25 Hz corresponding to first three transverse modes of the beam. Similarly, Figs. 3.6(a) and (b) show the frequency response curves of cantilever beams with three non-uniform sections with and without bolted joint. For the monolithic cantilever beam of three non-uniform sections without any bolted joints, the transverse modes are found at 7.25 Hz, 42.75 Hz, and 120.75 Hz. The corresponding frequencies of the cantilever beam with three non-uniform bolted sections are found at 5.625 Hz, 33.43 Hz, and 73.44 Hz, respectively. Comparison of results show that beam with bolted joints has lower modal frequencies than that of

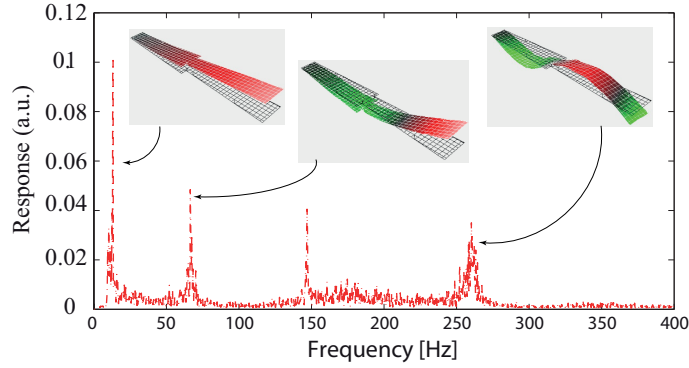Figure 3.5: Experimental frequency response of a bolted beam with two sections.

the monolithic beam due to reduction in stiffness at the joints. In the subsequent section, we first present the modeling of single non-uniform beam and monolithic three sections beam using ANSYS. Subsequently, we present analytical modeling of a single non-uniform beam and the bolted beam using lumped spring at the joint. The error associated with the measured values may vary from 0.25 to 1 Hz.

3.3 Numerical modelling and results

In this section, we present numerical modeling of single as well as monolithic non-uniform beams using 2D beam element in ANSYS. To model different sections, the cross-sections at $x = 0$ and $x = L$ are provided corresponding to the dimensions of single non-uniform beam. To model the beams of monolithic beam with three non-uniform sections, we provide six cross-sections corresponding to the ends of each section and glue them together. After providing the material properties of the beams, we perform modal analysis using block lancoz method to compute modal frequencies and corresponding modes of the single and bolted non-uniform beams. Figure 3.7(a), (b) and (c) show the numerically computed first three transverse mode shapes of non-uniform beam when smaller and wider ends are fixed, respectively. Similarly, we obtain the first three transverse modes of monolithic cantilever beam with three non-uniform sections as shown in Fig. 3.7(c). The frequency values of beams with single and three non-uniform sections are summerized in Table 3.2.

Table 3.2: Frequencies of cantilever beam with single and monolithic three non-uniform sections.

FEA models	1$^{\text{st}}$ mode	2$^{\text{nd}}$ mode	3$^{\text{rd}}$ mode
Single beam(Small end fixed)	54.49	380.75	1100
Single beam(Bigger end fixed)	74.30	419.22	1137.47
Three sections monolithic beam	6.64	41.88	118.43

On comparing the numerical results from Table 3.2 with the experimental results as mentioned in Table 3.1, we get very good agreement with a minimum and maximum percentage errors of 0.3% and 11%, respectively.
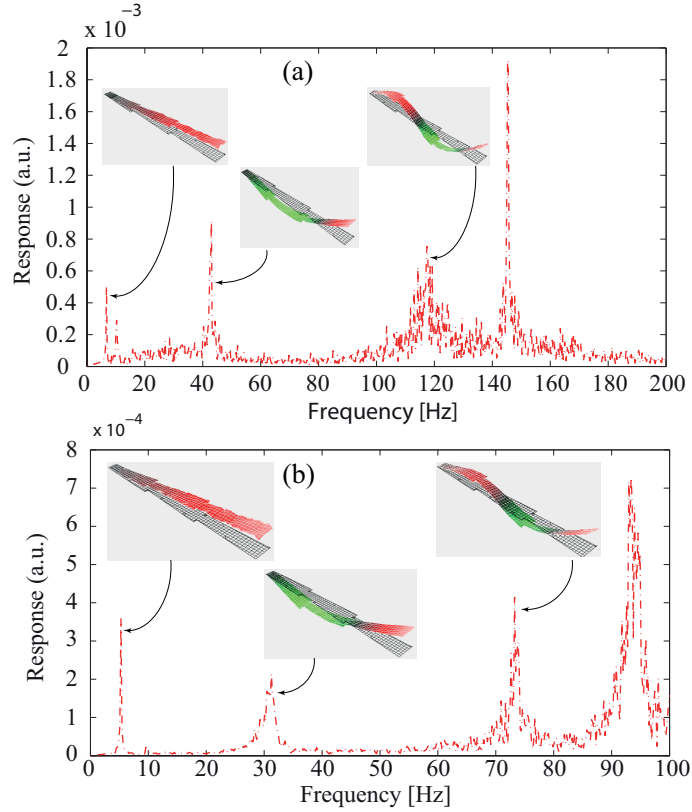
Figure 3.6: Experimental frequency response of a cantilever beam consisting of three non-uniform sections (a) without bolted joint, (b) with bolted joint.

3.4 Analytical procedure and results

In this section, we present approximate method to compute the first three transverse mode shapes of the single non-uniform cantilever beam with variable mass and elastic rigidity by following the approach proposed by Sarkar and Ganguli [25]. Later, we utilize the computed mode shape to obtain the modal frequencies using Rayleigh-Ritz method. After validating the method with the results of the single beams, separately, we compute the mode shapes and frequencies of bolted cantilever beams with two and three non-uniform sections, separately. We also compare the analytical results with experimental results for all the cases. The boundary conditions of the analytical model is formulated with the help of the analysis of experimental results. The analysis of experimental results helped us to identify the zero locations of the beams being tested for higher modes. The zero locations were incorporated in the boundary conditions and satisfied by the corresponding mode shape for the section.

3.4.1 Modal analysis of a single non-uniform beam

To compute the expression of mode shapes corresponding to first three transverse modes, we use zero positions from the measured mode shapes. Subsequently, we use the Rayleigh-Ritz method to compute the frequencies. Here, we apply this technique first for the single beam with linearly diverging section and then for the beam with linearly converging section from the fixed end.
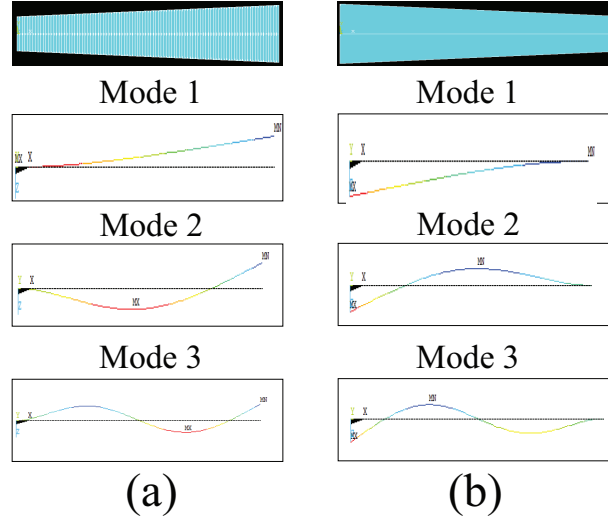
22

Figure 3.7: Finite element models and mode shapes of (a)single beam with diverging section, (b) single beam with converging section,

Non-uniform beam with diverging section

For a beam of length L, width $b_1 = 0.03$ m at the small end and $b_2 = 0.05$ m at the larger end, thickness, $h = 0.02$ m, the elastic modulus of $E = 69$ GPa and the density of $\rho = 2700$ kg/m^3, the transverse motion can be governed by the Euler-Bernoulli beam equation as [25],

$$\frac{\partial^2}{\partial x^2}\left(EI(x)\frac{\partial^2\phi}{\partial x^2}\right) - m(x)\omega^2\phi(x) = 0, \tag{3.2}$$

where, $\phi(x)$ is the unknown mode shape corresponding to the modal frequency ω which is obtained by satisfying the corresponding boundary conditions and the governing equation of the beam. Due to the variation of width along the length, the variation of mass $m(x)$ and the flexural rigidity $EI(x)$ can be obtained as

$$m(x) = 0.162 + 0.675x, \quad \text{and} \quad EI(x) = 1.38 + 5.75x. \tag{3.3}$$

After finding the approximate mode shape, we obtain the corresponding frequency using the Rayleigh-Ritz method as

$$\omega_n^2 = \frac{\sum_i \int_0^L \frac{\partial^2}{\partial x^2}\left(EI(x)_i\frac{\partial^2\phi_{ni}(x)}{\partial x^2}\right)\phi_{ni}(x)dx}{\sum \int_0^L m(x)_i\phi_{ni}^2(x)dx} \tag{3.4}$$

where, ω_n is the angular frequency and $f_n = \frac{\omega_n}{2\pi}$ is the frequency in Hz, ϕ_{ni} is the mode shape of ith section of the bolted beam corresponding to n^{th} mode and for the single beam, $i = 1$.

- *First Mode*: For the first mode of the single non-uniform cantilever beam, we approximate the assumed mode shape ϕ_{11} by a polynomial expression

$$\phi_{11}(x) = c_0 + c_1x + c_2x^2 + c_3x^3 + c_4x^4, \tag{3.5}$$

23

where, c_0, c_1, c_2, c_3, c_4 are five unknown coefficients. These unknowns are determined using the boundary conditions and normalization condition as follow.

$$\phi_{11}(0) = 0, \ \phi'_{11}(0) = 0, \phi''_{11}(L) = 0, \phi'''_{11}(L) = 0, \phi_{11}(L) = 1, \tag{3.6}$$

On solving the above equation, we obtain the following form of the first mode

$$\phi_{11}(x) = -390.62x^2 + 1627.60x^3 - 2543.13x^4. \tag{3.7}$$

Using Eqs. (3.4) and (3.7), we get the frequency of first mode as 54.52 Hz.

- *Second Mode*: By observing the second mode shape of single beam with lower end fixed from the experimental and numerical simulation from Figs. 3.2 and 3.7, we noticed that there exist an additional zero position at $\alpha = 0.1192$m from the fixed end. Consequently, the order of the assumed polynomial for the second mode shape is increased by one in order to satisfy additional zero position boundary condition. Therefore, the assumed mode shape can be written as

$$\phi_{21}(x) = c_0 + c_1 x + c_2 x^2 + c_3 x^3 + c_4 x^4 + c_5 x^5. \tag{3.8}$$

The unknown coefficients c_0, c_1, c_2, c_3, c_4, c_5 can be obtained from the following conditions:

$$\phi_{21}(0) = 0, \ \phi'_{21}(0) = 0, \phi''_{21}(L) = 0, \phi'''_{21}(L) = 0, \phi(\alpha) = 0, \phi_{21}(L) = 1 \tag{3.9}$$

where, $\alpha = 0.1192$ m is the zero-location of second mode. Solving the above equations, we obtain the final form of mode shape as

$$\phi_{21}(x) = -564.99x^2 + 9042.19x^3 - 45494.26x^4 + 78414.39x^5. \tag{3.10}$$

Using Eqs. (3.4) and (3.10), we get the frequency of first mode as 377.32 Hz.

- *Third Mode*: Like the case of second mode, by observing the modes of single beam from the experimental and numerical results as shown in Figs. 3.2 and 3.7, we noticed two additional zero locations at $\beta = 0.069$ and $\alpha = 0.128$ m from the fixed end. Consequently, the assumed mode shape can be approximated with the polynomial expression of order six, i.e., one order higher to the second mode to satisfy the extra zero conditions. The mode shape is given by

$$\phi_{31}(x) = c_0 + c_1 x + c_2 x^2 + c_3 x^3 + c_4 x^4 + c_5 x^5 + c_6 x^6 \tag{3.11}$$

The unknown coefficients c_0, c_1, c_2, c_3, c_4, c_5 and c_6 can be obtained from the following conditions:

$$\phi_{31}(0) = 0, \ \phi'_{31}(0) = 0, \phi''_{31}(L) = 0, \phi'''_{31}(L) = 0, \phi_{31}(\beta) = 0, \phi_{31}(\alpha) = 0,$$
$$\phi_{31}(L) = 1 \tag{3.12}$$

where, $\beta = 0.069$ and $\alpha = 0.128$ m are zero positions. On solving Eq. (3.12), we get the

following form of the mode shape

$$\phi_{31}(x) = 1249.98x^2 - 39521x^3 + 4.29 \times 10^5 x^4 - 1.95 \times 10^6 x^5$$
$$+5.23 \times 10^6 x^6. \tag{3.13}$$

Using Eqs. (3.4) and (3.13), we get the frequency of third mode as 947.5 Hz.

Table 3.3: Frequencies of single non-uniform beam with diverging section.

Modes	Exp. Result	Anal. Result	Num. Result
1st mode	54.68	54.42	54.49
2nd mode	371.09	377.32	380.75
3rd mode	1146.48	947.5	1100

On comparing the analytical solutions with the experimental and numerical results in Table 3.3, we found that the percentage errors of the first and second modes are less than 2% error and the third mode gives an error of about 17% with respect to the experimental results. The high error percentage in the third mode can be accredited to the high order of mode shape polynomial being used for the mode shape analysis. Also as the analytical boundary conditions are inspired by the experimental results which are subjected to real life conditions. In the analytical model we don't take into account the material damping and the fixture design which might also contribute to the natural frequency of the beam at higher modes.

Non-uniform beam with converging section

The next case is when the bigger cross section of the beam if fixed. As seen in the experimental case the first mode of the beam with the diverging section came very close to the beam with the converging section but there was significant difference in the frequency of the higher modes. The analytical model for the beam with converging section follows the same procedure but the only difference is in the mass and stiffness variation for the beam and the zero location boundary conditions. In the case of non-uniform beam with converging section from the fixed end, the variation of mass, $m(x)$ and the flexural rigidity, $EI(x)$ can be written as

$$m(x) = 0.675x + 0.270, \quad \text{and,} \quad \text{EI(x)} = 2.30 + 5.75\text{x}. \tag{3.14}$$

On observing the experimental and numerical mode shapes from Figs. 3.2 and 3.7, we found that the location of zero points in second and third modes remain the same as that of the uniform beam with diverging section. Therefore, the mode shapes obtained in the previous sections corresponding to all the three modes will remain the same. Using the mode shapes from Eqs. (3.7), (3.9) and (3.13), we computed the frequencies of first, second and third modes using Eq. (3.4). Finally, we compare the analytical values of modal frequencies with the numerical and experimental results in Table 3.4.

The table 3.4 shows the frequency comparison for the beam with the converging section obtained from the experimental, analytical and numerical result. The error in the first two modal frequencies is below 2% and the third frequency is having high error percentage. The reasons being same as explained in the previous section for the beam with diverging section.

Table 3.4: Frequencies of single non-uniform beam with converging section.

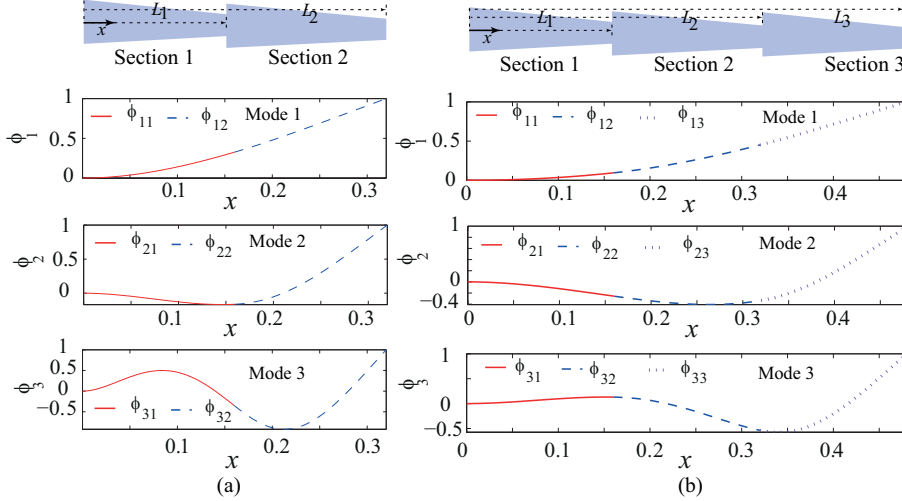| Modes	Exp. Result	Anal. Result	Num. Result
1st mode	66.40	57.50	74.30
2nd mode	401.36	395.66	419.22
3rd mode	1160.15	913.52	1137.47

Figure 3.8: Analytical mode shapes of bolted cantilever beams with (a) two, and (b) three non-uniform sections.

3.4.2 Modal analysis of a bolted cantilever beam with two non-uniform sections

After the experimental and analytical analysis of the individual non-uniform cantilever beams with converging and diverging sections we analysed an assembled beam comprising of two non-uniform beams and using a bolt to join them as an assembly. To analytically compute the mode shapes and frequencies of a bolted beam with two sections, we approximate the shape of each section by a polynomial of required order. The length of each section is taken as L=0.16 m such that first section ranges from $x = 0$ to $x = L_1 = 0.16$m and second section ranges from $x = L_1 = 0.16$ to $x = L_2 = 0.32$m. Using the dimensions and properties of the beam, the variation of mass and flexural rigidity for the two sections can be written as,

$$m_1(x) = 0.162 + 0.675x, \quad EI_1(x) = 1.38 + 5.75x.$$
$$m_2(x) = 0.054 + 0.675x, \quad EI_2(x) = 0.46 + 5.75x. \tag{3.15}$$

To find the frequencies of all the three modes, we first compute the mode shapes using approximate methods in conjunction with the boundary conditions, normalization condition and bolted joint condition, etc., in the following section.

- *First Mode*: The assumed first mode shape ϕ_1 is written in terms of the mode shapes of all the three sections, i.e., ϕ_{11} and ϕ_{12} such that $\phi_1 = \phi_{11} + \phi_{12}$. The assumed mode shapes of

26

ϕ_{11} and ϕ_{12}can be written as

$$\phi_{11}(x) = a_0 + a_1 \frac{x}{L} + a_2 \frac{x^2}{L^2},$$

$$\phi_{12}(x) = b_0 + b_1 \frac{x}{L} + b_2 \frac{x^2}{L^2} + b_3 \frac{x^3}{L^3} + b_4 \frac{x^4}{L^4} \tag{3.16}$$

where, a_0, a_1, a_2, b_0, b_1, b_2,b_3 and $b_4$are unknown coefficients which can be obtained from the boundary conditions, normalization conditions, and joint conditions. The equations associated with all the necessary conditions can be written as

$$\phi_{11}(0) = 0, \ \phi'_{11}(0) = 0, \ \phi_{11}(L_1) = \phi_{12}(L_1), \phi'_{11}(L_1) = \phi'_{12}(L_1),$$

$$(EI(x)\phi''_{11}(x))|_{x=L_1} = -k_{r1}\phi'_{11}(L_1)\,(EI(x)\phi''_{12}(x))|_{x=L_1},$$

$$\phi_{12}(L_2) = 1, \ \phi'''_{12}(L_2) = 0, \ \phi'''_{12}(L_2) = 0, (EI(x)\phi'''_{11}(x))|_{x=L_1} =$$

$$(EI(x)\phi'''_{12}(x))|_{x=L_1}, (EI(x)\phi'''_{12}(x))|_{x=L_2} = (EI(x)\phi'''_{13}(x))|_{x=L_2}, \tag{3.17}$$

where, k_{r1} is the torsional stiffness of the bolted joints located at $x = L_1$. The boundary conditions are of the fixed free beam. The value and the slope of the first section mode shape is equal to zero at the fixed location, and the value of shear force and bending moment is kept zero at the free end or the last point of beam for the third section. For the boundary conditions at the joint the value of mode shape and slope is made equal to each other. To involve the torsional spring effect we inducted the boundary condition where the moment is made equal for both section at the joint location. At the end to normalise the mode shape the end value is equal to one. Taking $k_{r1} = 0.01$ Nm/rad, the mode shapes of all the three sections corresponding to first mode of the bolted beam can be written as

$$\phi_{11}(x) = 16.35x^2 - 22.71x^3,$$

$$\phi_{12}(x) = 0.19 - 3.29x + 36.34x^2 - 75.70x^3 + 59.14x^4 \tag{3.18}$$

- *Second Mode*: On observing the second mode shape of bolted cantilever beam with two-single non-uniform sections obtained from the experimental result , we noticed that there exist an additional zero position at $x = \alpha = 0.21$ m which is located in second section. Consequently, the order of the assumed polynomial for the second section is increased by one in order to satisfy additional boundary condition, i.e., $\phi_{22}(\alpha) = 0$. Writing the second mode shape as $\phi_2 = \phi_{21} + \phi_{22}$, where, ϕ_{21} and ϕ_{22} are the assumed mode shapes of three sections which are represented the following polynomials

$$\phi_{21}(x) = a_0 + a_1 \frac{x}{L} + a_2 \frac{x^2}{L^2},$$

$$\phi_{22}(x) = b_0 + b_1 \frac{x}{L} + b_2 \frac{x^2}{L^2} + b_3 \frac{x^3}{L^3} + b_4 \frac{x^4}{L^4} + b_5 \frac{x^5}{L^5} \tag{3.19}$$

where, a_0, a_1, a_2, b_0, b_1, b_2,b_3, b_4 and b_5 are unknown coefficients which can be solved using the boundary conditions, normalization conditions, condition of additional zero position and

joint conditions which are given by

$$\phi_{21}(0) = 0, \ \phi'_{21}(0) = 0, \ \phi_{21}(L_1) = \phi_{22}(L_1), \phi'_{21}(L_1) = \phi'_{22}(L_1)$$
$$, (EI(x)\phi''_{21}(x))\,|_{x=L_1} = -k_{r1}\phi'_{21}(L_1)\,(EI(x)\phi''_{22}(x))\,|_{x=L_1},$$
$$\phi_{22}(L_2) = 1, \ \phi'''_{22}(L_2) = 0, \ \phi''_{22}(L_2) = 0, (EI(x)\phi'''_{21}(x))\,|_{x=L_1} =$$
$$(EI(x)\phi'''_{22}(x))\,|_{x=L_1}, (EI(x)\phi'''_{22}(x))\,|_{x=L_2} = (EI(x)\phi'''_{23}(x))\,|_{x=L_2}, \phi_{22}(\alpha) = 0, \quad (3.20)$$

Solving the above equations for the same values of k_1 we get the mode shapes corresponding to all the sections as

$$\phi_{21}(x) = -23.40x^2 + 106.68x^3,$$
$$\phi_{22}(x) = -1.59 + 46.81x - 526.86x^2 + 2581.64x^3 - 5495.07x^4$$
$$+ 4347.71x^5 + 31.52x^3 \quad (3.21)$$

Using Eqs. (3.4) and (3.21), we get the second modal frequency as 68.49 Hz.

- *Third Mode*: Similarly, on observing the modes of single beam from the experimental result as shown in Fig. 3.6(b), we noticed two additional zero locations at $x = \beta = 0.14$ and $x = \alpha = 0.28$ m from the fixed end. Consequently, the order of the assumed mode shape for the first section and the second section are increased by one order each as compared to that in the first mode. Consequently, the assumed mode shapes satisfy additional boundary conditions, i.e., $\phi_{31}(\beta) = 0$ and $\phi_{32}(\alpha) = 0$. Writing the third mode shape as $\phi_3 = \phi_{31} + \phi_{32}$, where, ϕ_{31} and ϕ_{32} are the assumed mode shapes of two sections which can be written as

$$\phi_{31}(x) = a_0 + a_1\frac{x}{L} + a_2\frac{x^2}{L^2} + a_3\frac{x^3}{L^3} + a_4\frac{x^4}{L^4},$$
$$\phi_{32}(x) = b_0 + b_1\frac{x}{L} + b_2\frac{x^2}{L^2} + b_3\frac{x^3}{L^3} + b_4\frac{x^4}{L^4} + b_5\frac{x^5}{L^5} \quad (3.22)$$

where, a_0, a_1, a_2, a_3, a_4, b_0, b_1, b_2, b_3, b_4, and b_5 are unknown coefficients which can be solved using the boundary conditions, normalization conditions, condition of additional zero position and joint conditions which are given by

$$\phi_{31}(0) = 0, \ \phi'_{31}(0) = 0, \ \phi_{31}(L_1) = \phi_{32}(L_1), \phi'_{31}(L_1) = \phi'_{32}(L_1)$$
$$, (EI(x)\phi''_{31}(x))\,|_{x=L_1} = -k_{r1}\phi'_{31}(L_1)\,(EI(x)\phi''_{32}(x))\,|_{x=L_1}, \ \phi_{32}(L_2) = 1,$$
$$\phi''_{32}(L_2) = 0, \ \phi'''_{32}(L_2) = 0, (EI(x)\phi'''_{31}(x))\,|_{x=L_1} = (EI(x)\phi'''_{32}(x))\,|_{x=L_1},$$
$$(EI(x)\phi'''_{32}(x))\,|_{x=L_2} = (EI(x)\phi'''_{33}(x))\,|_{x=L_2}, \phi_{22}(\alpha) = 0, \phi_{31}(\beta) = 0, \quad (3.23)$$

The mode shapes corresponding to two sections are,

$$\phi_{31}(x) = 266.20x^2 - 2967.18x^3 + 7612.58x^4,$$
$$\phi_{32}(x) = -27.24 + 675.76x - 6167.94x^2 + 2580.49x^3$$
$$+ 50665.90x^4 + 38087.75x^5 - 266.66x^3 + 354.59x^4 \quad (3.24)$$

Using Eqs. (3.4) and (3.24), we get the third modal frequency as 251.33 Hz.

Table 3.5: Frequency comparison for bolted beam with two sections

Mode	Exp. results	Anal. results	% Error
First mode	13.1	14.07	7.4
Second mode	66.5	68.49	3.0
Third mode	260.25	251.33	3.4

3.4.3 Modal analysis of a bolted cantilever beam with three non-uniform sections

To compute correct expression of mode shapes corresponding to first three modes of a bolted cantilever beam with three non-uniform sections, we capture the contribution of each section by different functions. To do the analysis, we take non-uniform sections with same length L, thickness t and varying width of b_1 to b_2 over a length of L as shown in Fig. 3.8. Section 1 is located from $x = 0$ to $x = L_1 = L$, section 2 is located from $x = L_1 = L$ to $x = L_2 = 2L$, and section 3 is from $x = L_2 = 2L$ to $x = L_3 = 3L$. Using the previously defined values of dimensions, the variation of mass, $m(x)$ and flexural rigidity $EI(x)$ over the three sections can be written as

$$m_1(x) = 0.162 + 0.675x, \quad EI_1(x) = 1.38 + 5.75x.$$
$$m_2(x) = 0.054 + 0.675x, \quad EI_2(x) = 0.46 + 5.75x. \tag{3.25}$$
$$m_3(x) = -0.054 + 0.675x, \quad EI_3(x) = -0.46 + 5.75x.$$

To find the mode shapes of first three modes of bolted beam with three non-uniform sections, we write the combined mode shape in terms of the shape of each section, respectively. Subsequently, we obtain the unknowns associated with the assumed mode shapes by satisfying the boundary conditions, normalization condition and the joint conditions.

- *First Mode*: The assumed first mode shape ϕ_1 is written in terms of the mode shapes of all the three sections, i.e., ϕ_{11}, ϕ_{12}, and ϕ_{13}, such that $\phi_1 = \phi_{11} + \phi_{12} + \phi_{13}$. The assumed mode shapes of ϕ_{11}, ϕ_{12}, and ϕ_{13} can be written as

$$\phi_{11}(x) = a_0 + a_1\frac{x}{L} + a_2\frac{x^2}{L^2}, \quad \phi_{12}(x) = b_0 + b_1\frac{x}{L} + b_2\frac{x^2}{L^2},$$
$$\phi_{13}(x) = c_0 + c_1\frac{x}{L} + c_2\frac{x^2}{L^2} + c_3\frac{x^3}{L^3} + c_4\frac{x^4}{L^4} \tag{3.26}$$

where, a_0, a_1, a_2, b_0, b_1, b_2, c_0, c_1, c_2, c_3 and c_4 are unknown coefficients which can be obtained from the boundary conditions, normalization conditions, and joint conditions. The equations associated with all the necessary conditions can be written as

$$\phi_{11}(0) = 0, \ \phi'_{11}(0) = 0, \ \phi_{11}(L_1) = \phi_{12}(L_1), \ \phi'_{11}(L_1) = \phi'_{12}(L_1),$$
$$(EI(x)\phi''_{11}(x))\,|_{x=L_1} = -k_{r1}\phi'_{11}(L_1) + (EI(x)\phi''_{12}(x))\,|_{x=L_1}, \ \phi_{12}(L_2)$$
$$= \phi_{13}(L_2), \ \phi'_{12}(L_2) = \phi'_{13}(L_2), (EI(x)\phi''_{12}(x))\,|_{x=L_2} = -k_{r2}\phi'_{12}(L_2)$$
$$+ (EI(x)\phi''_{13}(x))\,|_{x=L_2}, \ \phi_{13}(L_4) = 1, \ \phi''_{13}(L_4) = 0, \ \phi'''_{13}(L_4) = 0,$$
$$(EI(x)\phi'''_{11}(x))\,|_{x=L_1} = (EI(x)\phi'''_{12}(x))\,|_{x=L_1},$$
$$(EI(x)\phi'''_{12}(x))\,|_{x=L_2} = (EI(x)\phi'''_{13}(x))\,|_{x=L_2}, \tag{3.27}$$

where, k_{r1} and k_{r2} are the torsional stiffness of the bolted joints located at $x = L_1$ and $x = L_2$. Taking $k_{r1} = k_{r2}$=0.01, the mode shapes of all the three sections corresponding to first mode of the bolted beam can be written as

$$\phi_{11}(x) = 6.05x^2 - 5.04x^3, \ \phi_{12}(x) = 0.08 - 1.03x + 10.08x^2 - 8.40x^3,$$
$$\phi_{13}(x) = 0.63 - 6.48x + 30.26x^2 - 40.03x^3 + 21.89x^4 \tag{3.28}$$

and also shown in Figs. 3.8(b). Using Eqs. (3.4) and (3.28), we get the first mode frequency as 6.10 Hz.

- *Second Mode*: On observing the second mode shape of bolted cantilever beam with three-single non-uniform sections obtained from the experimental result as shown in Fig. 3.6(b), we noticed that there exist an additional zero position at $x = \alpha = 0.33$ m which is located in third section. Consequently, the order of the assumed polynomial for the third section is increased by one in order to satisfy additional boundary condition, i.e., $\phi_{23}(\alpha) = 0$. Writing the second mode shape as $\phi_2 = \phi_{21} + \phi_{22} + \phi_{23}$, where, ϕ_{21}, ϕ_{22}, and ϕ_{23} are the assumed mode shapes of three sections which are represented the following polynomials

$$\phi_{21}(x) = a_0 + a_1\frac{x}{L} + a_2\frac{x^2}{L^2}, \ \phi_{22}(x) = b_0 + b_1\frac{x}{L} + b_2\frac{x^2}{L^2},$$
$$\phi_{23}(x) = c_0 + c_1\frac{x}{L} + c_2\frac{x^2}{L^2} + c_3\frac{x^3}{L^3} + c_4\frac{x^4}{L^4} + c_5\frac{x^5}{L^5} \tag{3.29}$$

where, a_0, a_1, a_2, b_0, b_1, b_2, c_0, c_1, c_2, c_3, c_4 and c_5 are unknown coefficients which can be solved using the boundary conditions, normalization conditions, condition of additional zero position and joint conditions which are given by

$$\phi_{21}(0) = 0, \ \phi'_{21}(0) = 0, \ \phi_{21}(L_1) = \phi_{22}(L_1), \ \phi'_{21}(L_1) = \phi'_{22}(L_1),$$
$$(EI(x)\phi''_{21}(x))\,|_{x=L_1} = -k_{r1}\phi'_{21}(L_1) + (EI(x)\phi''_{22}(x))\,|_{x=L_1}, \ \phi_{22}(L_2)$$
$$= \phi_{23}(L_2), \ \phi'_{22}(L_2) = \phi'_{23}(L_2), (EI(x)\phi''_{22}(x))\,|_{x=L_2} = -k_{r2}\phi'_{22}(L_2)$$
$$+ (EI(x)\phi''_{23}(x))\,|_{x=L_2}, \ \phi_{23}(L_4) = 1, \ \phi''_{23}(L_4) = 0, \ \phi'''_{23}(L_4) = 0,$$
$$(EI(x)\phi'''_{21}(x))\,|_{x=L_1} = (EI(x)\phi'''_{22}(x))\,|_{x=L_1},$$
$$\phi_{23}(\alpha) = 0, \ (EI(x)\phi'''_{22}(x))\,|_{x=L_2} = (EI(x)\phi'''_{23}(x))\,|_{x=L_2}. \tag{3.30}$$

Solving the above equations for the same values of k_1 and k_2, we get the mode shapes corresponding to all the sections as

$$\phi_{21}(x) = -7.15x^2 + 18.91x^3, \ \phi_{22}(x) = -0.02 + 0.57x - 11.96x^2$$
$$+31.52x^3, \phi_{23}(x) = -16.24 + 231.18x - 1280.31x^2 + 3398.8x^3$$
$$-4302.38x^4 + 2110.14x^5. \tag{3.31}$$

The final second mode shape can also shown in Fig. 3.8(c). Using Eqs. (3.4) and (3.31), we get the second modal frequency as 38.38 Hz.

- *Third Mode*: Similarly, on observing the modes of single beam from the experimental result , we noticed two additional zero locations at $x = \beta = 0.23$ and $x = \alpha = 0.37$ m from the fixed end. Consequently, the order of the assumed mode shape for the second section and the third section are increased by one order each as compared to that in the first mode. Consequently, the assumed mode shapes satisfy additional boundary conditions, i.e., $\phi_{32}(\beta) = 0$ and $\phi_{33}(\alpha) = 0$. Writing the third mode shape as $\phi_3 = \phi_{31} + \phi_{32} + \phi_{33}$, where, ϕ_{31}, ϕ_{32}, and ϕ_{33} are the assumed mode shapes of three sections which can be written as

$$\phi_{31}(x) = a_0 + a_1\frac{x}{L} + a_2\frac{x^2}{L^2}, \ \ \phi_{32}(x) = b_0 + b_1\frac{x}{L} + b_2\frac{x^2}{L^2} + b_3\frac{x^3}{L^3},$$

$$\phi_{33}(x) = c_0 + c_1\frac{x}{L} + c_2\frac{x^2}{L^2} + c_3\frac{x^3}{L^3} + c_4\frac{x^4}{L^4} + c_5\frac{x^5}{L^5} \tag{3.32}$$

where, a_0, a_1, a_2, b_0, b_1, b_2, b_3, c_0, c_1, c_2, c_3, c_4, and c_5 are unknown coefficients which can be solved using the boundary conditions, normalization conditions, condition of additional zero position and joint conditions which are given by

$$\phi_{31}(0) = 0, \ \ \phi'_{31}(0) = 0, \ \ \phi_{31}(L_1) = \phi_{32}(L_1), \ \ \phi'_{31}(L_1) = \phi'_{32}(L_1),$$

$$(EI(x)\phi''_{31}(x))\,|_{x=L_1} = -k_{r1}\phi'_{31}(L_1) + (EI(x)\phi''_{32}(x))\,|_{x=L_1}, \ \ \phi_{32}(L_2)$$

$$= \phi_{33}(L_2), \ \ \phi'_{32}(L_2) = \phi'_{33}(L_2), (EI(x)\phi''_{32}(x))\,|_{x=L_2} = -k_{r2}\phi'_{32}(L_2)$$

$$+ (EI(x)\phi''_{33}(x))\,|_{x=L_2}, \ \ \phi_{33}(L_4) = 1, \ \ \phi''_{33}(L_4) = 0, \ \ \phi'''_{33}(L_4) = 0,$$

$$(EI(x)\phi'''_{31}(x))\,|_{x=L_1} = (EI(x)\phi'''_{32}(x))\,|_{x=L_1},$$

$$\phi_{32}(\beta) = 0, \ \ \phi_{33}(\alpha) = 0, \ \ (EI(x)\phi'''_{32}(x))\,|_{x=L_2} = (EI(x)\phi'''_{33}(x))\,|_{x=L_2}. \tag{3.33}$$

Solving the above equations using the same values of k_1 and k_2, we get the mode shapes corresponding to all the three sections as

$$\phi_{31}(x) = 5.77x^2 - 23.83x^3, \ \ \phi_{32}(x) = 0.2 - 5.82x + 64.1x^2$$

$$-266.66x^3 + 354.59x^4, \phi_{33}(x) = -54.50 + 736.71x - 3863.81x^2$$

$$+9796.72x^3 - 12024.83x^4 + 5768.64x^5. \tag{3.34}$$

The final second mode shape can also shown in Fig. 3.8(d). Using Eqs. (3.4) and (3.34), we get the second modal frequency as 91.88 Hz.

Finally, when we compare the analytical results with experimental results in Table 3.6, we find the maximum percentage error of about 15%. Error may be due to the approximate mode shapes, minor difference in the symmetry of the tapering and holes provided at the end of the fabricated non-uniform beams, some uncertainties associated with the bolted joints, frequency resolution in the measured signal, etc. It is also found that by increasing the torsional stiffness, we can obtain the changes in the mode shapes. Since the values of $k_{r1} = k_{r2} = 0.01$ are found to be small in the present case, therefore, modal frequencies of bolted beams may found to be closer to the monolithic beam with three sections without any bolted joints.

Table 3.6: Frequency comparison for bolted beam with three sections

Mode	Exp. results	Anal. results	% Error
First mode	5.63	6.10	8.35
Second mode	33.43	38.44	14.99
Third mode	73.44	74.97	2.0

Table 3.7: Frequency comparison for three section monolithic beam

Mode	Exp. results	Anal. results	% Error
First mode	6.75	6.10	9.63
Second mode	43.25	47.54	9.9
Third mode	118.0	110.55	6.74

3.4.4 Modal analysis of three-sections monolithic beam

In this section, we compute modal frequencies of monolithic beam with three sections without any joint by neglecting the terms associated with torsional stiffness at the joints. Using the zero position of second mode at $x = \alpha = 0.36$ and the third mode at $x = \alpha = 0.4$ and $x = \beta = 0.23$ obtained from the experimental mode shapes, we get the following form of the mode shapes using the same procedure as described in the previous section. For the first mode, we get the following shape functions

$$\phi_{11}(x) = 6.05x^2 - 5.04x^3, \ \phi_{12}(x) = 0.08 - 1.03x + 10.08x^2 - 8.40x^3,$$
$$\phi_{13}(x) = 0.63 - 6.48x + 30.25x^2 - 42.02x^3 + 21.89x^4. \tag{3.35}$$

For the second mode, we obtain the mode shape as

$$\phi_{21}(x) = -10.50x^2 + 24.98x^3, \ \phi_{22}(x) = -0.04 + 0.96x - 17.50x^2 + 41.62x^3,$$
$$\phi_{23}(x) = -20.49 + 291.00x - 1610.05x^2 + 4264.21x^3 - 5389.75x^4 + 2640.77x^5. \tag{3.36}$$

Similarly, the corresponding mode shapes for the third mode are obtained as,

$$\phi_{31}(x) = 11.56x^2 - 47.53x^3, \ \phi_{32}(x) = 0.33 - 9.82x + 110.99x^2 - 461.40x^3$$
$$+597.17x^4, \phi_{33}(x) = -84.59 + 1137.73x - 5935.53x^2 + 14972.72x^3$$
$$-18312.23x^4 + 8761.62x^5 \tag{3.37}$$

Using the mode shape expressions, we obtained the modal frequencies from Eq. (3.4) as 6.10 Hz, 47.54 Hz, and 118.0 Hz corresponding to first three transverse modes. On comparing the analytical results with the experimental results as mentioned in Table 3.7, the percentage errors are found to be below 10%.It is also noticed that due to small values of torsional stiffness at the joints, the first mode frequency is found to be same as that of the bolted beam. At the outset, we state that the method presented in the paper can be easily extended to the bolted beams of several complicated bolted non-uniform sections where the stiffness of the bolted joint is significant.

3.5 Summary

The study in this chapter presents the modal analysis of non-uniform beams with cantilever configuration. The beams studied are single non-uniform beam with diverging section, single non-uniform beam with converging section, two section bolted beams, three section monolithic beam and finally three section bolted beams. Experiments are conducted on all beams with the help of vibrometer and the frequency response graph is acquired. The frequency at which transverse modes are obtained is acquired. The experimental result also gave information about the torsional modes for the beam. The results are then verified with the help of analytical model following approximate mode shape approach as used in the previous chapter. The boundary conditions used take care of the fixed end and other end free. Also the bolted beam is represented by the torsional stiffness as in the previous chapter for the simply supported beam configuration. The mode shape polynomial were altered according to the modified boundary conditions for the corresponding modes. The modification in the boundary condition in contrast to previous chapter which was based on numerical model was based on the experimental results. The mode shape expression were then used to obtain natural frequencies with the help of Rayleigh-Ritz method.

The results obtained for the bolted section beams from the experimental and analytical result show a maximum error of 15%. The use of approximate mode shape instead of exact mode shape approach can be a reason for this discrepancy. Also the difference between the values obtained can be accounted to the real life conditions in which the experiment is conducted. The beam is fixed on a fixture that has its own natural frequencies and hence it affects the frequency of the specimen. The material damping and the bolted damping effect is also found in the experimental measurements which is assumed to be negligible in the analytical model.

Chapter 4

Numerical Analysis of bolted beams

In this chapter we present the numerical modeling of bolted beams. The study is initiated with a two section non-uniform beam bolted together and later the study is extended to three section non-uniform bolted cantilever beam. First three fundamental modes are extracted and the analysis is done for the number of elements and the effect of value of torsional stiffness of bolted joint "k" on the frequency.

4.1 Numerical procedure

Direct modeling method is used for modeling bolted beams. The study is initialised with defining nodes. Separate nodes are defined at bolted connection for the coupling element along with the node present at the joint. Next step is to assign the material properties to the elements. The Young's modulus of rigidity is taken as, $E = 69e9$ Nm/rad^2, density,$\rho = 2700$ kg/m^3 and poisson's ratio as $\mu = 0.3$. After this step the real constant are defined in which area, inertia and the thickness of the section is provided. The elements are assigned to material properties after this step. The element taken for the study is "BEAM3".

- BEAM3 is a uniaxial element with tension, compression, and bending capabilities. The element has three degrees of freedom at each node: translations in the nodal x and y directions and rotation about the nodal z-axis.

While assigning elements to material properties it is important to note that at the joint the connection is to be made between the separate node and the next node located on other beam not the node of the previous beam. The bolted joint is treated as a spring with torsional stiffness. For this the element used is "COMBIN14" which is a spring damper model element.

- COMBIN14 has longitudinal or torsional capability in one, two, or three dimensional applications. The longitudinal spring-damper option is a uniaxial tension-compression element with up to three degrees of freedom at each node: translations in the nodal x, y, and z directions. No bending or torsion is considered. The torsional spring-damper option is a purely rotational

element with three degrees of freedom at each node: rotations about the nodal x, y, and z axes. No bending or axial loads are considered.

For our case we have considered normally loaded joint hence the damping effect can be neglected. Hence, we have only provided value for the element stiffness and not for the damping constant. This element is defined between the nodes at same location. For our case we have considered different values of "k" and analysed the result. The last step is to assign mass to the elements. The mass is calculated for each element length and assigned with the help of MASS21 element.

- MASS21 is a point element having up to six degrees of freedom: translations in the nodal x, y, and z directions and rotations about the nodal x, y, and z axes. A different mass and rotary inertia may be assigned to each coordinate direction.

The mass for each element is found by the expression,

$$m(x) = (\rho)b(x)hl \tag{4.1}$$

where, $'b(x)'$ is the variation of breadth along the beam. The height $'h'$ remains constant for the whole beam and $'l'$ is the length of the element. The length decreases as the number of elements is increased.

The analysis is done for varying values of $'k'$ and then the convergence of the results is analysed by increasing the elements.

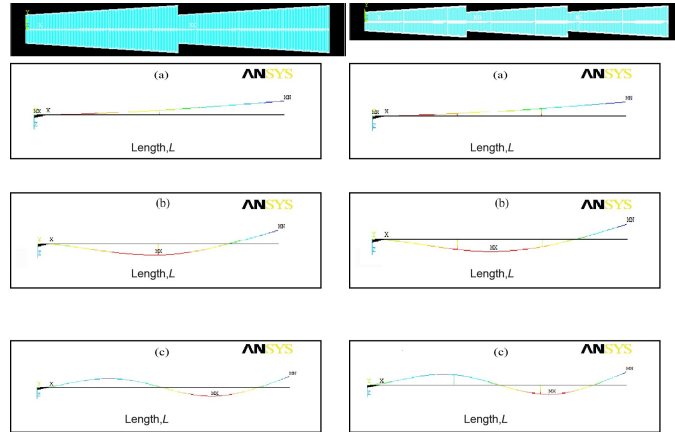Figure 4.1: Finite element models and mode shapes of (A)two section beams, (B)three section beams,

4.2 Numerical results

The modal analysis is done using Block Lancoz method. First three vibrational modes are extracted for each beam for which the results are shown in Fig. 4.1. Fig. 4.1 (A) shows the modes obtained for the two section bolted beam and (B) shows the modes obtained for three section bolted beam.

4.2.1   Effect of variation of 'k'

The aim of the analytical model for our study is to find an optimised value of stiffness $'k'$ for which the frequency difference is minimum for all three modes compared to experimentally obtained frequency. In the similar way we tried to study the effect of stiffness on the numerical model. The values of $'k'$ are varied, and the results are as shown in Table. 4.1. For the study we have divided the three beam into 24 elements. The Table. 4.1 shows that the frequency decreases with the value of $'k'$. The value of $'k'$ for which the error is minimised is $'k' = 8$. The numerical study shows the effect of the bolted joint stiffness on the beams. The use of torsional spring stiffness as a element for bolted joint is proved to be effective. The frequencies also depend on the number of elements taken in the beam. As we increase the number of elements the result comes in close proximity of analytical and experimental results.

Table 4.1: Frequency comparison for three section bolted beam based on stiffness variation

'k'	1st mode	2nd mode	3rd mode
100	6.89	48.56	115.41
50	6.24	42.57	108.74
20	6.22	37.24	93.31
15	6.035	35.86	87.42
12	5.86	34.68	82.67
10	5.71	33.66	78.12
8	5.52	32.35	73.97
5	4.12	29.74	64.75

4.3   Summary

In this chapter we presented the numerical analysis of the bolted beams with two and three sections respectively. The effect of variation of torsional stiffness 'k' was studied using COMBIN14 element. The frequencies were found to be closer to experimental and analytical results at a smaller value of 'k'.

Chapter 5

Conclusion and future work

This thesis presents work on studying vibrational behaviour of non-uniform beams in different configuration such as simply supported and cantilever beam. Closed form solutions or approximate mode shape are formulated for the analytical study. The study is first done on beams with simply supported configuration. We first analytically computed the results for the first mode by following the closed solution approach and then compared the result with numerical results obtained using ANSYS. Subsequently, we extended the method to compute the mode shapes and frequencies of second and third modes of a single non-uniform beam and compare the results with numerical results. Finally, we extend the analytical and numerical methods to compute the mode shapes and frequencies of three non-uniform beams bolted together to form a long simply-supported beam. On comparing the results, we found reasonable match of the analytically computed results with the numerical results. For the next stage we study non-uniform beams with cantilever configuration.
To develop the model, we first carry out experiments to measure the modal frequencies and shapes for single as well as bolted non-uniform beams. On comparing the results, we found that the frequencies of bolted beams reduce due to reduction in the stiffness at the joints as compared to that of the monolithic beam with three sections without joints. To understand the modeling, we also develop numerical models of cantilever beams with single and three non-uniform sections without joint. On comparing the numerical and experimental results, we found that the model based on the Euler-Bernoulli beams can be used to develop analytical model. Finally, we develop approximate analytical model to first find the mode shapes using the information of zero position of the experimental mode shapes for the single beam and then compare the results with the experimental and numerical values. Subsequently, we extend the method to model the bolted beams by replacing each bolted joint by a torsional spring of stiffness, $k_r = 0.01\text{Nm/rad}$. On comparing the analytical results with experiment values, we found the maximum percentage error of about 15% in found in the bolted beam with three non-uniform sections. For the case of bolted beam with two sections, the percentage error is found to be less than 10%. The error may be due to the approximate mode shapes as well as differences in the physical dimensions of fabricated non-uniform beams. Finally, we state that the method presented in this thesis can be easily extended to the bolted structures with many non-uniform sections.The work can be extended to introduce non-linearity in the vibration. Non-linear stiffness term can be modified to the existing governing equation for study of non-linear behaviour.

References

[1] D. Platus. Aero elastic stability of slender, spinning missiles. *Journal of Guidance* 15, (1992) 144–151.

[2] S. Pradhan and P. Datta. Dynamic instability characteristics of a free-free missile structure under a controlled follower force. *Aircraft Engineering and Aerospace Technology* 78-6, (2006) 509–514.

[3] A. K. Gupta. Vibration of tapered beams. *Journal of Structural Engineering* 111(1), (1985) 19–36.

[4] S. Abrate. Vibration of Non-uniform rods and beams. *Journal of Sound and Vibration* 185(4), (1995) 703–716.

[5] J.Wu and C.Ho. Analysis Of wave-induced horizontal-and-torsional-coupled vibrations of a ship Hull. *Aircraft Engineering and Aerospace Technology* 31-4, (1987) 235–252.

[6] S. H. Pourtakdoust and N. Assadian. Investigation of thrust effect on the vibrational characteristics of flexible guided missiles. *Journal of Sound and Vibration* 272(1-2), (2004) 287–299.

[7] J. W. Jaworski and E. D. Dowell. Free vibration of a cantilevered beam with multiple steps: Comparison of several theoretical methods with experiment. *Journal of Sound and Vibration* 312(4-5), (2008) 713–725.

[8] D. Zheng, Y. Cheung, A. Francis, and Y. Cheng. Vibration of multi-span non-uniform beams under moving loads by using modified beam vibration functions. *Journal of Sound and Vibration* 2112(3), (1998) 455–467.

[9] L. Gaul and R. Nitsche. The Role of Friction in Mechanical Joints. *Applied Mechanics Reviews* 54(2), (2001) 93–106.

[10] S. Bograd, P. Reuss, A. Schmidt, L. Gaul, and M. Mayer. Modeling the dynamics of mechanical joints. *Mechanical Systems and Signal Processing* 25(8), (2011) 28012826.

[11] M. Oldfield, H. Ouyang, and J. Mottershead. Simplified models of bolted joints under harmonic loading. *Computers and Structures* 84, (2005) 25–33.

[12] M. Todd, J. Nichols, and L. Virgin. An assessment of modal property effectiveness in detecting bolted joint degradation: theory and experiment. *Journal of Sound and Vibration* 275(3-5), (2004) 1113–1126.

[13] H. Ouyang, O. M.J, and M. J.E. Experimental and theoretical studies of a bolted joint excited by a torsional dynamic load. *International Journal of Mechanical Sciences* 48, (2006) 1447–1455.

[14] X. Ma, L. Bergman, and A. Vakakis. Identification of bolted joints through laser vibrometry. *Journal of Sound and Vibration* 246(3), (2001) 441460.

[15] C. J. Hartwigsen, Y. Song, D. M. McFarland, L. A. Bergman, and A. F. Vakakis. Experimental study of non-linear effects in a typical shear lap joint configuration. *Journal of Sound and Vibration* 277, (2004) 327351.

[16] D. Quinn. Modal analysis of jointed structures. *Journal of Sound and Vibration* 331(1), (2012) 81–93.

[17] S. Tol and H. Ozguven. Dynamic characterization of bolted joints using FRF decoupling and optimization. *Mechanical Systems and Signal Processing* 54-55, (2004) 124–138.

[18] D. Chen and J. Wu. The exact solutions for the natural frequencies and mode shapes of non-uniform beams with multiple spring mass systems. *Journal of Sound and Vibration* 255(2), (2002) 299–322.

[19] Y. Song, C. Hartwigsen, D. Macfarland, A. Vakakis, and L. Bergman. Simulation of dynamics of beam structures with bolted joints using adjusted Iwan beam elements. *Journal of Sound and Vibration* 273, (2004) 249–276.

[20] M. Eriten, M. Kurt, G. Luo, D. M. McFarland, L. A. Bergman, and A. F. Vakakis. Nonlinear system identification of frictional effects in a beam with a bolted joint connection. *Mechanical Systems and Signal Processing* 39, (2013) 245–264.

[21] H. Ahmadian and H. Jalali. Generic element formulation for modelling bolted lap joints. *Mechanical Systems and Signal Processing* 21(5), (2007) 2318–2334.

[22] D. S and K. Willner. Investigation of a jointed friction oscillator using the Multiharmonic Balance Method. *Mechanical Systems and Signal Processing* 52-53, (2015) 73–87.

[23] V. Jaumouille, J. Sinou, and B. Petitjean. An adaptive harmonic balance method for predicting the nonlinear dynamic responses of mechanical systems Application to bolted structures. *Journal of Sound and Vibration* 329, (2010) 4048–4067.

[24] R. Ibrahim and C. Pettit. Uncertainties and dynamic problems of bolted joints and other fasteners. *Journal of Sound and Vibration* 279, (2005) 857–936.

[25] K. Sarkar and R. Ganguli. Closed-form solutions for non-uniform Euler Bernoulli free free beams. *Journal of Sound and Vibration* 332, (2013) 6078–6092.

[26] P. F. Pai and S. Y. Lee. Non-linear structural dynamics characterization using a scanning laser vibrometer. *Journal of Sound and Vibration* 264, (2003) 657–687.

[27] M. Amabili and S. Carra. Experiments and simulations for large-amplitude vibrations of rectangular plates carrying concentrated masses. *Journal of Sound and Vibration* 331, (2012) 155–166.